Deciphering the Function of HAM1 in the Biology of Cryptococcus neoformans Item

Elizabeth Arsenault Yee

Publication Date

21-12-2023

DECIPHERING THE FUNCTION OF *HAM1* IN THE BIOLOGY OF *CRYPTOCOCCUS NEOFORMANS*

A Dissertation

Submitted to the Graduate School

of the University of Notre Dame

in Partial Fulfillment of the Requirements

for the Degree of

Doctor of Philosophy

by

Elizabeth Arsenault Yee

_____

Felipe H Santiago Tirado, Director

Graduate Program in Biological Sciences

Notre Dame, Indiana

December 2023

DECIPHERING THE FUNCTION OF *HAM1* IN THE BIOLOGY OF *CRYPTOCOCCUS NEOFORMANS*

Abstract

by

Elizabeth Arsenault Yee

Cryptococcus neoformans is a global fungal pathogen that primarily impacts immunocompromised individuals. Responsible for ~200,000 yearly cases in the HIV+ population, and a mortality rate as high as 81%, this devastating pathogen remains a significant global health issue mostly due to ineffective antifungals and an incomplete understanding of pathogenesis. By characterizing genes with connections to virulence we may be able to uncover new pathways for more targeted treatments.

We previously described a cryptococcal palmitoyl transferase important for virulence. One of its main substrates is the protein encoded by the uncharacterized gene CNAG_02129. This gene has a partially characterized homolog in the filamentous fungus *Neurospora crassa* named *HAM13,* where it plays a role in proper cellular communication and fusion of fungal filaments. In *Cryptococcus*, cellular communication is essential during mating, therefore we hypothesized that CNAG_02129, which we have named *HAM1,* may play a role in mating. Here we have shown that *ham1*Δ mutants produce more progeny during mating and filament more robustly which are all consistent

with a role in mating. When looking at pheromone transcription using qPCR, we found that our *ham1*Δα cross trended towards higher MATα and MATa pheromone expression suggesting that *HAM1* is acting as a negative regulator of mating. When looking at *HAM1* transcription overtime, likewise, we saw trends of low expression early on in the mating cycle with higher expression at later time points, again lending support to the idea that *HAM1* may be acting as a negative regulator or checkpoint in mating. Moreover, our *ham1*Δα exhibits a competitive fitness defect under mating and non-mating conditions which suggests that there may be additional defects in other important biological aspects such as virulence.

Consistent with the notion that mating and virulence are linked, we have found several differences with the major virulence factor, the polysaccharide capsule, of our *ham1*Δ strains. *ham1*Δ mutants exhibit defects with capsular release and transfer, and shed more exopolysaccharide under certain conditions relative to wild-type (WT). When virulence was tested in an *in vivo* model, we were surprised to find that there was no significant difference in the survival of *ham1*Δ infected and WT infected *G. mellonella* larvae. When investigating the fungal burden at time of death we also found no difference between the *ham1*Δ and WT infected larvae.

Fungal mating is a vital part of the lifecycle of the pathogenic yeast *C. neoformans*. More than just ensuring the propagation of the species, mating allows for genetic diversity as well as the generation of infectious particles that can invade mammalian hosts. Despite its importance in the biology of this pathogen, we still do not know all of the major players regulating the mating process and if they are involved or

impact its pathogenesis. Understanding the connection between mating and virulence through the study of *HAM1* dysfunction may open new avenues of investigation into ways to improve the treatment of this disease.

I dedicate this thesis to my family and my wonderful husband Chris - thank you for believing in me, I would not be here without you.

CONTENTS

FIGURES

ACKNOWLEDGEMENTS

I owe a lot of gratitude to so many people so I will do my best to put it into words. My path to science was an interesting one, starting in the 4th grade with a diorama about the humble seahorse. My teacher, Mrs. Cavicci came up to me at the school science fair and said “have you ever thought about being a marine biologist?” That question stuck with me and led me to pursuing opportunities at the New England Aquarium to declaring a major in Marine Sciences at the University of Connecticut.

While in college, I met two very influential people that inspired me to keep pursuing learning, Dr. Claudia Koerting (my MARN mom) and Dr. Michael Finneguera (Evo Devo professor-extrodinare and the reason why I got a minor). Without their support in college, (literally letting me skip class to take a job interview) and beyond with recommendations and looking at applications I might not be sitting here today writing this.

After college, I really won the lottery with first jobs. While intimidating at first, the Roche Molecular Solutions family welcomed me with open arms especially my departmental manager Dr. Yu Tian. When I went into Yu’s office to break the news that I had gotten into graduate school he said “of course you did, we will miss you here but it’s important you go.” Since then, he has been a friend, mentor and supporter of all my accomplishments, for that I cannot thank you enough.

When I hit grad school I started as a Masters student at the University of Connecticut, that’s where I met Dr. Glenn Milton, my then graduate student advisor.

Glenn took me under his wing in the midst of trying to finish his dissertation and on the brink of having his first baby answering all my questions with patience and kindness. Glenn, thank you for teaching me how to be a mentor and even now taking the time to answer my dumb science questions and sending me memes to cheer me up or cheer me on.

Then came the Irish. I started my PhD at the University of Notre Dame. Here I met my advisor Dr. Felipe Santiago-Tirado. I have honestly never met someone more excited about science or The Last of Us. Jokes aside, thank you Felipe for helping me become the scientist I am today and for letting me pursue this wacky world of fungal mating. For that I am truly thankful. One of the cool things about being first, is you get to see a lab grow around you. To my two OG lab mates Pete and Chris thank you for helping me build this lab from the ground up and being with me on this crazy journey. To the newbies, Robbi and Gina while our time together was short thank you for joining the Santiago-Tirado family, I know I am leaving the lab in good hands with you at the helm.

What's grad school without friends you might ask? I wouldn't know because I have some of the best friends around. To the Grillapalooza gang (Kurt, Alyssa, Marissa, Michael and so many others), thank you for all the laughs, burgers, brats and beers over the years. Our weekly hangs have been a bright spot in my time here. They say that good friends will keep up with you when you move away but true friends will come and visit. Thank you for the many trips you have made my dear Caitlin (and the new kid on the block Andy) I can't wait to use all my frequent flyer miles to see you in Detroit.

Now for the people that have always been in my corner, my family. My mom Meg, my dad Phil, my brother Peter. Thank you for picking up the phone no matter the time of day or night to either tell me “not to quit” or to rejoice with me in my accomplishments. I appreciate your support and love more than you know. Also, to my new family, my wonderful in-laws Barbara and Hon, thank you for lending me your son for a few years out here in Indiana and for cheering me on.

To my wonderful husband Chris, you have supported me in anything I have wanted to do since our first date back in 2015. From flying out to see me every few months, to moving in with me during the Pandemic, to getting married last year, I love doing life with you. Thank you for always being here for me.

Finally, I would like to give a special thanks to my nana. She was so excited about me coming to Notre Dame to start my PhD and would always say “that’s my granddaughter she’s getting her Doctorate at Notre Dame”. I hope I’ve made you proud because your little girl is graduating as a Fighting Irish.

CHAPTER 1:

INTRODUCTION

1.1 Overview

1.1.1 What is Cryptococcus neoformans?

Cryptococcus was first identified in 1894 by German pathologist Otto Busse and surgeon Abraham Buschkle. They isolated a "*Saccharomyces*-like" organism from a young woman who was suffering from a bone infection (Srikanta et al., 2014, Busse, 1894). In the same year, Francesco Sanfelice reported isolating a similar yeast organism from fermenting peach juice which he called *Saccharomyces neoformans* due to its unique colony forming structure (Srikanta et al., 2014, Sanfelice 1894). Finally, in 1901 French mycologist Jean Paul Vuillemin renamed the organism *Cryptococcus neoformans* (*C. neoformans*) due to the fact that it does not produce ascospores which is a defining characteristic of the *Saccharomyces* genus (Srikanta et al., 2014).

Documented cryptococcosis cases remained low throughout the 1900s until the 1980s during the AIDS epidemic (Srikanta et al., 2014). It's estimated that 80% of cryptococcosis patients were HIV+ during this time and even today is still a leading cause of death in this population (Mazairz and Perfect, 2016, Rajasingham et al., 2022). For several decades the causative agents of cryptococcosis were classified as two varieties that included 5 serotypes. These were *C. neoformans var neoformans* serotypes A, D, and AD, and *C. neoformans var gatti* serotypes B and C (Kwong-Chung et al., 2014). With

the improvement of genomic and molecular approaches, the taxonomy of *Cryptococcus* has been reaccommodated to include 7 distinct species and hybrids (Hagen et al., 2015). The previous *C. neoformans var neoformans* was separated into 2 species (*C. neoformans* and *C. deneoformans*) and a hybrid (*C. neoformans* x *deneoformans*), and *C. neoformans var gatti* into 5 species. Hence, all serotype A strains are now *C. neoformans* and all serotype D are *C. deneoformans*. Interestingly, there is a clear difference between *C. neoformans* and *C. deneoformans* in their potential to cause infection and propensity to mate (Lin et al., 2008, Barchiesi et al., 2005). *C. neoformans* comprise 95% of clinical isolates and have been associated with higher virulence potential in animal models as compared to *C. deneoformans* (Lin, 2008, Barchiesi et al., 2005). Additionally, the majority of these isolates are of the MATα background (Rosen et al., 2013, Bicanic et al., 2009, Montoya et al., 2021). At the same time, whereas *C. deneoformans* is amenable to mating, *C. neoformans* exhibits very poor mating efficiency. *Cryptococcus* undergoes a bisexual mating cycle involving two sexes that are defined by their MAT loci designated MATα and MATa which will be described later in this chapter (Sun et al., 2019).

Regardless of the infectious strain, individuals come in contact with *C. neoformans* in the environment. Associated with bird guano, tree bark and soil, desiccated yeast and spores are inhaled into the lungs and, in immunocompetent individuals, the infection is controlled and individuals remain asymptomatic until the fungus is cleared (Maziarz and Perfect, 2016). However, in immunocompromised individuals, fungal cells can quickly overwhelm the immune system in the lungs resulting in pneumonia and acute respiratory distress syndrome (Maziarz and Perfect, 2016).

Fungal cells can then disseminate to the central nervous system causing lethal meningoencephalitis (Maziarz and Perfect, 2016).

As a leading cause of death in individuals that are HIV+ cases are well documented in this population, with approximately 152,000 cases in 2020 with 112,000 resulting in death (Rajasingham et al., 2022). This staggering mortality rate stems largely from a lack of effective treatment options as well as an incomplete understanding of cryptococcal pathogenesis. With the rise of many fungal infections across the world, recently the World Health Organization published its first Fungal Pathogen Priority List to raise awareness for fungal infections (World Health Organization, 2022). *Cryptococcus neoformans* was categorized as the top position in the highest critical priority group on this list, driving home the need for a better understanding of this pathogen (World Health Organization, 2022).

1.1.2 Identification of *PFA4* as necessary for complete pathogenesis

Cryptococcal-immune cell interactions are critical for disease establishment and progression and will influence the outcome of the infection (Kwon-Chung et al., 2014). Immune cells phagocytose fungal cells in an effort to clear the infection but in fact, depending on the immune status of the host, become a safe haven for the fungus and even the vehicle that *C. neoformans* uses to move to new areas within a host (Kwon-Chung et al., 2014).

Clinical data has shown that increased phagocytosis of *C. neoformans* leads to worse patient outcomes and higher fungal burden in cerebrospinal fluid (Sabitti et al., 2014, Alanio et al., 2011, Pham et al., 2023). To determine what fungal factors are

necessary for phagocyte recognition and internalization, our lab conducted a screen of 1,201 single deletion mutants looking for differences in phagocytosis (Santiago-Tirado et al., 2015). One of the top mutants consistently exhibiting higher levels of phagocytosis was 2A12, a homolog of *Saccharomyces cerevisiae*'s Protein Fatty Acyltransferase 4 (*PFA4*) (Santiago-Tirado et al., 2015). Palmitoyl acyl transferases (PATs) are enzymes that catalyze the post translational modification palmitoylation by adding palmitic acid moieties to substrate proteins. This results in a conformational change in the target protein resulting in a higher affinity for membranes (Nichols et al., 2015).

Characterization of the cryptococcal *pfa4*Δ resulted in several phenotypes that most likely contributed to its higher phagocytic index, including a collapsed cellular morphology, alterations in exposure of cell wall components, and sensitivity to various cellular stressors (Santiago-Tirado et al., 2015). Most notably, *pfa4*Δ mutants were unable to cause disease in a mouse model and as such is necessary for complete virulence in *C. neoformans* (Santiago-Tirado et al., 2015).

1.2 Post translational modifications and their role in disease

An important process in eukaryotic cell biology is the use of post translational modifications (PTMs) (Retanal et al., 2021, Salomon and Orth 2013). PTMs are the addition of functional groups to proteins either covalently or non-covalently, altering the protein's function by changing the physical and chemical properties (Retanal et al., 2021, Salomon and Orth 2013). This allows for target proteins to accomplish specific functions and/or the structural capability to drive foundational processes within the cell (Retanal et al., 2021, Salomon and Orth 2013). In the context of infectious disease, host cells rely on PTMs to deliver proteins to their correct locations and are crucial to fundamental

biological processes like stress response, growth/division, cell-to-cell signaling and many others (Retanal et al., 2021, Salomon and Orth 2013).

One strategy employed by pathogens to establish themselves in a host is to hijack PTM machinery to modify their own proteins or create enzymes to inhibit target protein modifications. One of the first reported virulence enzymes to catalyze a host PTM was diptheria toxin produced by the pathogenic bacteria *Corynebacterium diphtheriae* (Salomon and Orth 2013, Gill et al., 1969, Honjo et al., 1968). Since this discovery in the late 1960s, multiple groups have described virulence proteins that mediate PTMs (Salomon and Orth., 2013) While the contribution of PTMs to host invasion by viruses and bacteria have been studied extensively, our understanding of their role in pathogenic fungi is very limited (Retanal et al., 2021, Salomon and Orth 2013, Sobocinska, J et al., 2017).

1.2.1 Palmitoylation in Fungi

One PTM that was of particular interest to us based on our previous findings with *PFA4* was palmitoylation. Palmitoylation is a reversible post translational modification where the saturated fatty acid palmitic acid (C16:O) is added to free cysteine residues of a target protein via a thioester bond (Sobocińska, J et al., 2017, Nichols et al., 2015). This process is catalyzed by a protein palmitoyl acyl transferase (PAT) and results in the target protein having a higher affinity for membranes (Sobocińska, J et al., 2017, Nichols et al., 2015). The reversible nature of this process differentiates palmitoylation from other constitutive PTM's such as prenylation and allows for dynamic localization of target proteins (Nichols et al., 2015). In fungi, the first PAT genes were identified in *S.*

cerevisiae as the enzymes responsible for palmitoylation of Ras1 (Erf2) and yeast casein 1 (Akr1) (Nichols et al., 2015, Lobo et al., 2002, Roth et al., 2002).

In *C.* neoformans, palmitoylation of Ras1 and subsequent plasma membrane attachment are essential for the maintenance of normal morphology and pathogenicity (Nichols et al., 2009, Nichols et al., 2015). With this evidence that palmitoylated proteins are part of cryptococcal pathogenesis and our finding that *PFA4* was necessary for complete virulence, we wanted to identify downstream targets of Pfa4 to gain a better understanding of the proteins it modifies and what processes they may be involved in (Santiago-Tirado et al., 2015). To determine the Pfa4 palmitoylome, we coupled metabolic labeling of palmitoylated proteins using alk-16 (an analogue of palmitate) with a pulldown with streptavidin beads to specifically capture palmitoylated proteins in WT and *pfa4*Δ cells (Santiago-Tirado et al., 2015). We then used these purified protein fractions in a comparative mass spectrometry approach to see what proteins were enriched in WT samples over *pfa4*Δ samples, resulting in the first palmitoylome of any fungal pathogen (Santiago-Tirado et al., 2015).

1.3 Bipolar mating systems in Fungi and the MAT loci

Sexual reproduction and determination are usually dictated by sex chromosomes, but in fungi it is controlled by the mating-type loci (MAT). First molecularly characterized in *S. cerevisiae*, distinct MATα and MATa sequences encode transcription factors that permit the pheromone, receptor genes as well as other factors to be transcribed in a mating-type specific way (Mate 2002). Basidiomycete fungi can be one of two mating systems: bipolar or tetrapolar (Hsueh and Heitman, 2008). Bipolar systems

have a single MAT locus contained within one cell whereas tetrapolar have two unlinked MAT loci within a cell (Hsueh and Heitman, 2008, James et al., 2006).

A possible reason for having two systems lies in the exchange of genetic material during a mating interaction (Hsueh and Heitman, 2008, James et al., 2006). In order for successful mating to occur, the two parents must be compatible at the MAT loci (Hsueh and Heitman, 2008, James et al., 2006). These parents can be derived from two different sources, either mating between siblings (inbreeding) or mating between a progeny from one cross with another from the broader population (outcrossing) (Hsueh and Heitman, 2008). In a bipolar system the potential for inbreeding is higher because 50% of full sibling progeny are mating compatible whereas only 25% of tetrapolar siblings are compatible (Hsueh and Heitman, 2008, James et al., 2006).

1.3.1 Overview of the mating cycle in *C. neoformans*

C. neoformans has a bipolar mating system which can undergo both unisexual and bisexual reproduction (Hsueh and Heitman, 2008, Sun et al., 2019) In environmental conditions that are mating permissive, *C. neoformans* will begin secreting small lipid modified peptides known as pheromones. These pheromones are mating specific to either MATα or MATa cells (Sun et al., 2019). These pheromones then bind to G-protein coupled receptors (GPCRs) that are specific to the mating type of the recipient cell, Ste3α and Ste3a (Sun et al., 2019, Shen et al., 2002). Pheromone binding to GPCRs results in activation of the pheromone response pathway which is composed of a mitogen activated protein kinase (MAP-K) cascade (Sun et al., 2019). This MAP-K cascade results in activation of the transcription factor Mat2, which both directly and indirectly regulates

expression of the MAT locus (Sun et al., 2019). Once activated, the MAT locus orchestrates a complex signaling network of several transcription factors that control various aspects of the morphological component of the mating process (Sun et al., 2019).

Following activation of the pheromone response pathway, cryptococcal cells will undergo morphological changes akin to the schmooing process observed in *S. cerevisiae* (McClelland et al., 2004, Kwon-Chung et al., 2014, Fu and Heitman, 2017). Cells of the MATα mating type respond to pheromone by forming conjugation tubes while the MATa cells become enlarged, possibly to increase the area available to fuse with the conjugation tube (Wickes et al., 2002).

After this cellular fusion event, a diploid zygote is produced that then undergoes a morphological transition into a filamentous form called a heterokaryotic dikaryon because each segment of the hypha contains two distinct nuclei (Sun et al., 2019, Gyawali and Lin 2011, Lin, 2009). This form also has clamp cells connecting neighboring hyphal compartments which ensure inheritance of the two parental nuclei in each hyphal segment and that they remain independent nuclei until the formation of the basidium (Gyawali and Lin 2011, Lin, 2009). Once the heterokaryotic dikaryon reaches the appropriate length, the hyphal tip differentiates into the globose basidium, where the two parental nuclei fuse and undergo meiosis to produce four haploid meiotic daughter nuclei (Sun et al., 2019, Lin 2009). These four daughter nuclei then undergo several rounds of mitosis to produce four linear chains of basidiospores (Sun et al., 2019, Lin 2009).

Due to the predominance of the MATα background in environmental and clinical isolates it was thought that *C. neoformans* underwent asexual reproduction rather than

unisexual mating (Roach et al., 2014). Studies looking closely at the populations of these MATα cells have shown that *C. neoformans* has developed a self-fertile strategy allowing them to reproduce unisexually (Roach et al., 2014). Unisexual reproduction involves the same activation of the pheromone response pathway however the filamentous structure that is produced is exclusively monokaryotic and the clamp cells along these monokaryotic filaments remain unfused, allowing for fusion of the two parental nuclei prior to or at the basidium (Roach et al., 2014, Gyawali et al 2011). What is important to note about unisexual reproduction is that it has only been observed in *C. deneoformans* and well documented in the laboratory strain JEC21 but not in *C. neoformans* (Fu et al., 2014).

1.2.2 Importance of mating to *C. neoformans*

Beyond the need for reproduction to carry on the species, mating in *C. neoformans* is necessary for virulence. The haploid spores that result from mating interactions are the infectious agents inhaled by mammalian hosts (Sun et al., 2019). Spores are 1-2μm in size and as such are ideal for alveolar deposition and have a higher tolerance to external stressors such as oxidative stress, high temperatures, chemical attacks and desiccation (Botts and Hull, 2010, Botts et al., 2009).

In addition to being better at alveolar deposition, the interaction of spores with the surrounding lung environment is different than with yeast (Sun et al., 2019). Yeast cells cannot be phagocytosed by macrophages without opsonization (Sun et al., 2019, Alvarez and Casadevall 2006). Conversely, spores are readily phagocytosed in the absence of opsonins and survive within the macrophage environment eventually germinating into

yeast cells (Sun et al., 2019, Botts et al., 2009). These yeast cells are in turn able to mitotically divide within the macrophage and disseminate to the central nervous system (Sun et al., 2019).

1.4 Morphology and Virulence

With the discovery of the mating cycle of *C. neoformans*, we know that cells can have one of three different morphological states: yeast, hyphae and spores. We know that both the yeast and spore forms can establish infection in a mammalian host but, contrary to its infectious counterparts, the hyphal form of *C. neoformans* is unable to cause disease (Alvarez and Casadevall 2006, Botts et al., 2009, Lin 2009). Besides the obvious difference in the morphology of the hyphal form there is a distinct difference in the immune response triggered by the hyphal form when compared to the yeast form in a mammalian host (Zhai et al., 2015).

1.4.1 The immune response of a mammalian host to Cryptococcal infection

The surface of yeast and hyphal cells is distinct, and expose antigens that elicit different immune responses. These differential responses depend on the type of helper T lymphocytes (Th cells) that are activated by the antigens (Mukaremera and Nielsen 2017). These Th cells can have three different responses to fungal pathogens: Th cell type 1 (Th1) can produce a pro-inflammatory response that kills intracellular pathogens, Th cell type 2 (Th2) produce an anti-inflammatory response promoting antibody, eosinophilic and other cell-mediated responses against helminths, and Th cell type 17 (Th17) which are associated with mucosal immunity and autoimmune diseases (Mukaremera and Nielsen 2017, Berger 2000). The type of Th response mounted will

determine the activation of the macrophage populations, from pro-inflammatory, or M1, to anti-inflammatory, or M2. Notably, a Th2 response will counteract a Th1 mediated response resulting in a different overall immune outcome (Berger 2000).

It is known from both animal and clinical data that cryptococcal infections result in a Th2 immune response and M2 macrophage polarization (Wagner et al., 2015). This Th2 response results in increased fungal burden, dissemination, and exacerbation of disease (Wagner et al., 2015). On the contrary, a Th1 response and M1 polarization leads to fungal clearance and fungicidal activity (Nelson et al., 2020). This is well documented for infections with the yeast form (Lin 2009). However, infections with the hyphal form result in a Th1 immune response, with M1 macrophages that are able to destroy the fungus. This was tested using a cryptococcal strain constitutively overexpressing the hyphal regulator Znf2 (*ZNF2*^{OE}), which results in cells in pseudo hyphal or elongated forms (Lin et al., 2010, Zhai et al., 2015). Therefore, the yeast form provides advantages for disease establishment and progression. Moreover, not only these hyphal-locked cells cannot cause disease, but upon reinfection with a highly virulent WT fungus, the animals were protected. This highlights the potential use of the filamentous form of *C. neoformans* as a vaccine strategy (Zhai et al., 2015).

1.4.2 Vaccine strategies using filamentous morphology

Investigations into generating a vaccine against cryptococcal infection have been comprehensively studied for years but no strategies have succeeded past the pre-clinical research phase (Normile and Del Poeta., 2023). The lack of vaccine advancement is primarily due to the sensitive population that is predominantly affected by *C. neoformans*

infections and the struggles they face with their immune systems (Normile and Del Poeta., 2023). As a result, vaccine formulations exhibiting high efficiency in animal models that are immunodeficient are of great interest to the fungal community (Normile and Del Poeta., 2023).

The observation that *ZNF2*^{OE} could be used as a vaccine strategy prompted a subsequent investigation to test if it would work under immunocompromised conditions (Pham et al., 2023). In this study, not only the authors showed that the live-vaccine regiment tested by Zhai et al. in 2015 provides long-term protection, but also provides protection against a second challenge months after recovery of the initial challenge (Pham et al., 2023). Because of these promising results, the investigators tested if using a heat-killed *ZNF2*^{OE} would provide protection in a mouse model that had a depleted CD4+ T cell population, mimicking the immune profile of HIV+ individuals. This resulted in extended survival without extrapulmonary dissemination, and the extend of the protection was dependent on the mouse breed. Because the live-vaccine always outperformed the heat-killed strategy, next the authors introduced a mutation in the *ZNF2*^{OE} background that renders it completely incapable of causing disease, even in the absence of T cells. Usage of this modified strain resulted in improved protection in animals depleted for CD4+ T cells (Pham et al., 2023).

This exciting discovery that the filamentous morphology of *C. neoformans* provides not only immunity to challenges with virulent strains of *Cryptococcus* but also effectively prevents dissemination reveals a new avenue to target cryptococcal disease. With the extensive similarities to well defined mating pathways in other fungal organisms, it is a system that often gets overlooked for new therapeutic targets. We have

only begun to scratch the surface of the complexities of cryptococcal biology with respect to mating and its connection to virulence but there is a pressing need for a better understanding of this necessary cellular process and the players involved.

CHAPTER 2:

HAM1 ACTS A NEGATIVE REGULATOR OF MATING

2.1 Abstract[1]

We previously described a cryptococcal palmitoyl transferase important for virulence. One of its main substrates is the protein product encoded by the uncharacterized gene CNAG_02129. This gene has a partially characterized homolog in the filamentous fungus *Neurospora crassa* named *HAM13,* where it plays a role in proper cellular communication and filament fusion. In *Cryptococcus*, cellular communication is essential during mating, therefore we hypothesized that CNAG_02129, which we have named *HAM1,* may play a role in mating.

We have found that *ham1Δ* mutants produce more progeny in a mating interaction, and create hyphae more robustly indicative of some role in the mating pathway. When we examined pheromone transcription via qPCR, we observed in our *ham1*Δα unilateral and bilateral crosses higher trends of MATα transcription over time. This provides further confidence for our mating hypothesis and suggests that it may be acting as a negative regulator of mating. We also examined *HAM1* transcription over time, and found that *HAM1* transcript was low at the earliest time point but that this was reversed at later time points of the mating cycle. Finally, when assessing competitive

[1] This chapter contains work that is currently under review at Microbiology Spectrum. To access the preprint please see this citation: Yee, E. A., Ross, R. L., & Santiago-Tirado, F. H. (2023). Phenotypic characterization of *HAM1*, a novel mating regulator of the fungal pathogen *Cryptococcus neoformans*. *bioRxiv*, 2023.2009.2018.558251. https://doi.org/10.1101/2023.09.18.558251

fitness, we observed a significant difference between *ham1*Δ mutants depending on the MAT background. Our *ham1*Δα exhibited competitive fitness defects under mating and non-mating conditions whereas our *ham1*Δa exhibited no defects. Overall, our results are consistent with *HAM1* acting as a negative regulator of mating, and suggests that *HAM1* dysfunction affects vegetative growth as well.

2.2 Introduction

When examining the downstream targets of Pfa4 we saw that there were several candidate proteins that were involved in cell wall synthesis, membrane trafficking, and signal transduction (Santiago-Tirado et al., 2015). However, one of the most highly enriched targets in WT over *pfa4*Δ samples was encoded by the gene of unknown function CNAG_02129. From our BLAST analysis, this gene is unique for the fungal kingdom and its only homolog that was partially characterized was found in the filamentous ascomycete *Neurospora crassa*. This homolog was named hyphal anastomosis protein 13 (*HAM-13*) because it was found in a screen for mutants that could not undergo hyphal fusion (Dettmann et al., 2014).

Briefly, *N. crassa* produces large quantities of clonal spores that when they land on a suitable substrate germinate into structures called germlings which chemotropically grow towards each other to make contact. These germlings then undergo cellular fusion and mature into interconnected hyphae to form a mycelium (Fischer et al., 2019). In the *ham-13*Δ mutant these resultant spores were only able to find each other and fuse 33% of the time, demonstrating a large defect on cellular communication (Dettmann et al., 2014). Many of the other mutants identified were part of the MAK-2 mitogen-activated protein kinase (MAPK) cascade, and it was speculated that *HAM-13* may play a role in that pathway as well. This MAK-2 cascade is analogous to the MAPK mating pathway in *S. cerevisiae*. This MAPK cascade is conserved across many pathogenic fungi containing bipolar mating systems such as *Aspergillus fumigatus*, *Candida albicans,* and *C. neoformans* (Lin, 2010, Raudaskoski, 2010, Szewczyk and Krappmann 2010). With this

in mind, we wanted to investigate if CNAG_02129 could have a function in cryptococcal mating.

In our study, we determined that CNAG_02129 which we have named *HAM1* (Hyphal anastomosis protein 1), plays a role in cryptococcal mating by acting as a negative regulator of the mating process. With our *ham1*Δ strains we found increased cellular fusion with and without exogenous pheromone, a hyper hyphal response during bisexual mating scenarios, trends of differences in MATα pheromone loci expression over time in unilateral and bilateral crosses, and differential *HAM1* transcription throughout the mating cycle. Finally, we found significant differences in competitive fitness of our *ham1*Δ mutants depending on the MAT background. Our *ham1*Δα had reduced competitive fitness in both mating and non-mating conditions whereas our *ham1*Δa mutant exhibited no defects.

Notably, we only saw these phenotypes in *C. neoformans* (serotype A) and not in *C. deneoformans* (serotype D). *C. deneoformans* is much more prone to mating and can undergo both bisexual and unisexual mating, hence it is more amenable to mating studies than *C. neoformans*. By characterizing the role of *HAM1* in fungal mating we have not only uncovered a novel player in the mating cycle, but this discovery also highlights the differences in mating regulation between the sister species of *C. neoformans* and *C. deneoformans*.

2.3 Results

2.3.1 Ham1 is a palmitoylated protein conserved across the fungal kingdom.

In order to look for *HAM1* homologs we constructed a phylogenetic tree to see if it was conserved in the fungal kingdom exclusively or if there were cross kingdom hits. We found that not only is *HAM1* a fungal kingdom-specific gene, but that it is closely conserved in the cryptococcal family and several other pathogenic fungal species (Figure 1.1 A). This finding could prove useful if there is a connection between *HAM1* and virulence as a possible new avenue to target for a broad-spectrum antifungal treatment.

Next, to confirm the results of our previous large scale Pfa4 palmitoylome studies, we investigated the palmitoylation status of Ham1. Using a Ham1-FLAG tagged strain we performed an immunoprecipitation coupled with click-chemistry to determine if the Ham1 protein was palmitoylated. We either "fed" or did not feed ("unfed") fungal cultures with alk-16, an analog of palmitate, as indicated by the + and – signs in the Figure 1.1B. By using these fractions, we are able to confirm that our click-chemistry reaction was successful by the absence of fluorescent banding in the unfed fraction. We successfully confirm that Ham1 is palmitoylated by the presence of a fluorescent band only in the fed fraction of our Ham1-FLAG IP, that was at the same size as the accompanying western blot (Fig 1.1 B, C). As a result of this finding, we wanted to see if the palmitoylation modification may be conserved across the protein homologs. Using the palmitoylation predictor software GPS-Palm (Ning et al., 2020), we determined that all of the homologs investigated through our phylogeny analysis had very high confidence predictions for palmitoylation (Fig 1.1 D).

Figure 1.1 Ham1 is a palmitoylated protein conserved across the fungal kingdom. A) Phylogenetic tree showing conserved homologs of CNAG_02129 across fungal species. The evolutionary history of the sequences was inferred using the Maximum Likelihood method with MEGAX software (Tamura et al., 2021). The tree with the highest log likelihood (-10358.64) is shown. 1,000 replicate analyses (bootstraps) were run and the percentage of trees in which the associated taxa clustered together is shown next to the branches. B) Immunoprecipitation (IP) pull down of palmitoylated Ham1 using click chemistry. Cells were either fed or not fed with alk-16, an analog of palmitate (as indicated by the + and – symbols in the figure to designate fed vs unfed) then lysed and underwent protein extraction. An IP was then performed on fed and unfed fractions coupled with a Click chemistry experiment highlighting palmitoylated proteins. C) An accompanying western blot was run on the remaining fraction not used for click chemistry. Ham1-FLAG is 908 aa (~100 KDa) highlighted ladder lanes are 100 and 130 KDa respectively. D) Predicted palmitoylation scores of homologs found in pathogenic fungal species using GPS-Palm (Ning et al., 2020) and the partially characterized homolog found in N. crassa. Threshold cutoff for GPS palm was set to low to look at all predicted palmitoylation sites (>0.6484).

A

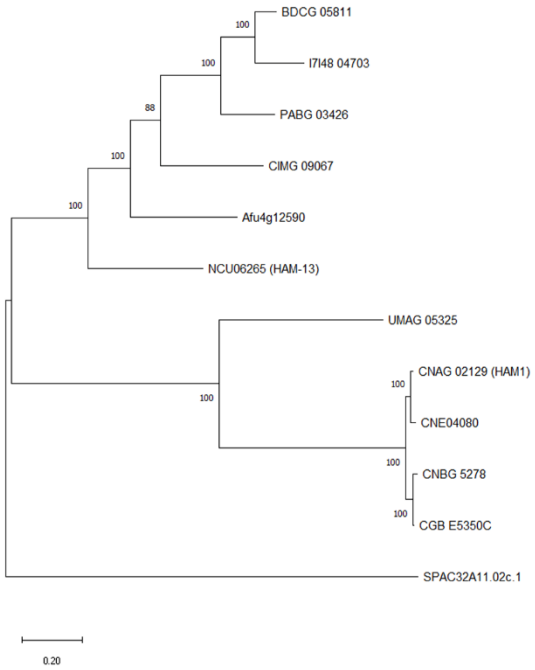

B

C

D

Species Name	Fungi DB Acession Number	Predicted Palmitoyation Sites	Confidence Score
Cryptococcus neoformans H99	CNAG_02129	395 559	0.878 0.775
Cryptococus deneoformans JEC21	CNE_04080	395	0.878
Cryptococcus gatti WM267	CGB_E5350C	395 559	0.878 0.775
Kwoniella bestiolae CBS 1018	I302_06570	391	0.810
Aspergillus fumigatus Af293	Afug12590	41 75	0.741 0.830
Histoplasma capsulatum G217B	I7I48_04263	400	0.809
Paracoccidioides brasiliensis Pb03	PABG_03426	400	0.894
Coccidiodies immitis RS	CIMG_09067	377	0.651
Blastomyces dermatitis ER-3	BDCG_05811	400	0.881
Ustilago maydis 521	UMAG_05325	312 410	0.837 0.819
Neurospora crassa OR74A	NCU06265	38 442	0.682 0.820

2.3.2 *ham1*Δ exhibits altered cellular fusion and progeny with a dry colony morphology.

The goal of mating is to produce viable progeny with traits from both parents, generating better-adapted cells (Fu et al., 2019). This requires that parental strains find each other, fuse, undergo recombination, and then produce haploid spores (Fu et al., 2019). To test if mating was affected, deletion strains of *HAM1* were generated in the KN99 background (WT) with either MATα or MATa mating loci using different resistance markers (G418 or NAT). To see if our *ham1*Δ mutants can produce recombinant viable progeny we set up mating crosses between KN99α x KN99a, KN99a x *ham1*Δα, and KN99α x *ham1*Δa, and determine the fusion efficiency from the number of colonies resistant to both antibiotics. Both *ham1*Δ mutant crosses yielded significantly higher progeny resistant to both antibiotics when compared to the WT cross, indicating faster, or more efficient, cellular fusion (Fig. 1.2 A, Fig. 1.8B).

To explore the impact that pheromone has on cellular fusion we tested if adding synthetic exogenous pheromone would increase the rate of cell fusion in our *ham1*Δ mutants. In the KN99a x *ham1*Δα cross, cellular fusion increased in a dose dependent manner, whereas in the KN99α x *ham1*Δa cross, fusion events went up slightly with increasing pheromone until reaching a plateau at 7.5μM (Fig. 1.2 A, Fig. 1.3 B, C). When we looked at the individual crosses more closely, we found that in the WT cross there was an increase in the number of progeny generated by adding exogenous pheromone but there was no significant difference in the fusion rate (Fig. 1.3). In our *ham1*Δα cross we saw a significant increase in progeny at 7.5μM exogenous pheromone with additional trends towards significance in both 5 and 10μM (Fig 1.3 B). In our *ham1*Δa cross we observed a similar increase in progeny at 7.5μM ($p=0.06$) and trends towards significance at 5 and

10μM (Figure 1.3). This suggests that the *ham1*Δ crosses are more sensitive to exogenous pheromone.

Interestingly, when scoring double-resistant progeny, we observed a difference in the colony morphology. Rather than the typical glossy, round shape colonies of WT strains, our *ham1*Δ progeny had a dry, irregular morphology (Fig. 1.2 B). When resuspending single colonies from these crosses and staining them with DAPI and CFW to visualize nuclei and cell wall, respectively, we found that these colonies were comprised of the hyphal form of *Cryptococcus,* as the septal divisions and a bi-nuclear distribution along septa were evident (Fig. 1.2B). In contrast, the colonies from the WT crosses only showed budding yeasts. This drastic increase in the ability to fuse as well as the dry appearance and hyphal state of *ham1*Δ progeny led us to consider what other facets of the mating cycle could be altered.

Figure 1.2 *ham1*Δ mutants have higher cellular fusion efficiency and exhibit dry colony morphology A) Percent double antibiotic progeny resulting from bisexual crosses. 2-way ANOVA with a Dunnet's multiple comparison test of WT fusion to *ham1*Δα and *ham1*Δa in no pheromone and exogenous pheromone conditions ** p= 0.0012, *** p= 0.0009, **** p<0.0001 n=3 biological replicates for all crosses and all conditions. B) Representative images of colony body of all crosses at 2x magnification and 100x magnification of progeny staining with Calcofluor white (CFW) to highlight septal divisions of hyphal form in mutant crosses DAPI to show binuclear distribution in mutant crosses. Scale bars represent 50 and 10 microns, respectively.

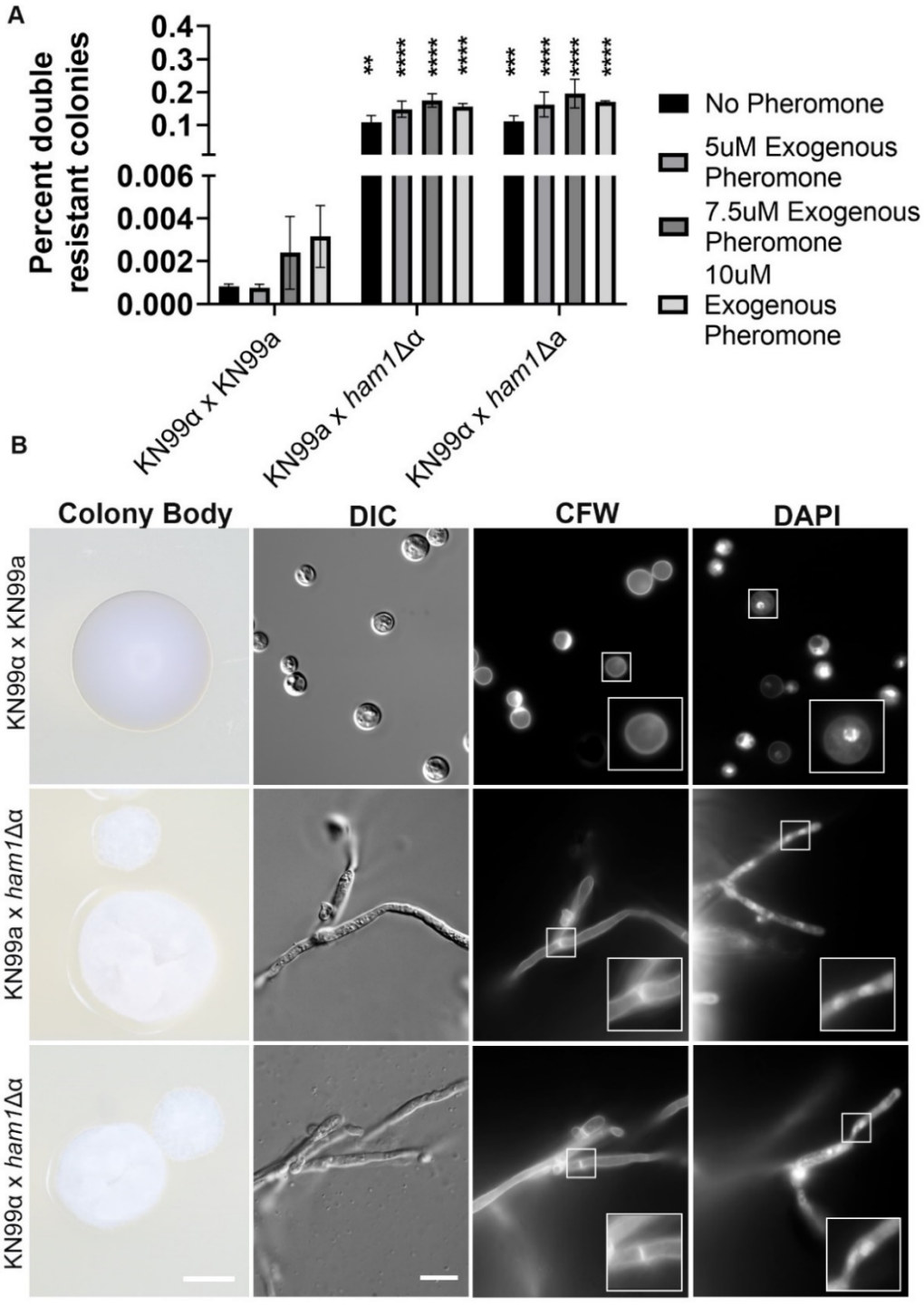
A
Percent double resistant colonies
0.4
0.3
0.2
0.1
0.006
0.004
0.002
0.000
**
****
****
****
***
****
****
****
No Pheromone
5uM Exogenous Pheromone
7.5uM Exogenous Pheromone
10uM Exogenous Pheromone
KN99α x KN99a
KN99a x ham1Δα
KN99α x ham1Δa
B
Colony Body
DIC
CFW
DAPI
KN99α x KN99a
KN99a x ham1Δα
KN99α x ham1Δα

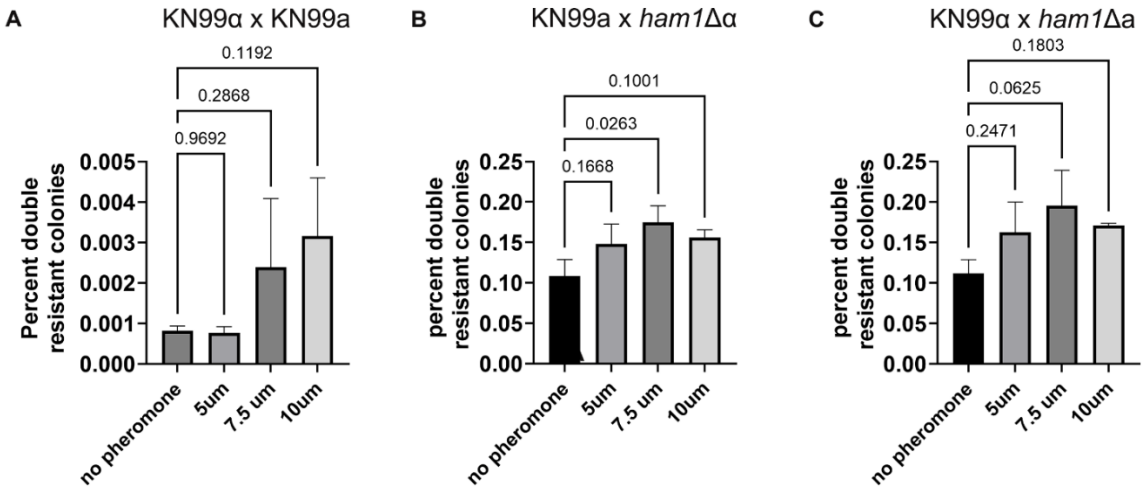

Figure 1.3 Cellular fusion comparisons of no pheromone and pheromone conditions in individual crosses. A) WT cell fusion without and with 5µM, 7.5µM, and 10µM exogenous pheromone. A One-way ANOVA with an LSD Fisher's test was run on all conditions. P values for each condition are shown. B) *ham1*Δα cell fusion without and with 5µM, 7.5µM, and 10µM exogenous pheromone. A One-way ANOVA with an LSD Fisher's test was run on all conditions. P values for each condition are shown. The 7.5µM condition was found to be significantly different from the no pheromone condition $p < 0.05$. C) *ham1*Δa cell fusion without and with 5µM, 7.5µM, and 10µM exogenous pheromone. A One-way ANOVA with an LSD Fisher's test was run on all conditions. P values for each condition are shown. n= 3 biological replicates per condition for all cell fusion assays.

2.3.3 *ham1*Δ mutants have increased hyphal production in bisexual mating scenarios only on V8 medium.

Hyphal growth is a quantitative trait that can be used to measure how well a strain is able to mate (Fu et al., 2019). We assessed the ability of our *ham1*Δ crosses to form hyphae in a time course from 5 days to 4 weeks, under V8 media. We observed more robust and faster hyphal formation in our *ham1Δ* crosses across all time points (Fig. 1.4A, Figure 1.8A). When quantifying the hyphal area, we observed a significant increase in all unilateral mutant crosses at 5 days and 3 weeks, and a significant increase in the hyphal area of the bilateral cross across all time points (Fig 1.4B).

Although V8 media is the most common media used in *C. neoformans*, other mating media has been used successfully in other *Cryptococcus* species. Murashige-Skoog media (MS media) was first discovered as a suitable media for mating assays during a study of the interaction between *Cryptococcus* spp. and plants (Xue et al., 2007). Cryptococcal cells of both *C. neoformans* and *C. deneoformans* strains were spotted together in a bisexual mating interaction on MS media and produced hyphae and mating structures after 4 weeks of incubation (Xue et al., 2007).

As a result, MS media has continued to be used as an additional mating media. Filamentation agar (FA) was initially generated to look at alternative carbon source usage (Xu et al., 2017). It was found that replacing the traditional glucose used in Yeast-Peptone (YP) media with glucosamine stimulated mating structure formation in the various species tested (Xu et al., 2017). Since these additional mating medias were fairly simple to generate, we decided to test our *ham1*Δ mutants on these medias to see if the hyper-hyphal phenotype was consistent across diverse mating medias. We observed no

significant increase in the hyphal area generated during bisexual mating scenarios across our time course in either MS media (Fig 1.6 A-C) or in FA (Fig. 1.6 D-F).

Figure 1.4 *ham1*Δ unilateral and bilateral crosses exhibit increased hyphal production on V8 mating medium in a time course. A) Representative images of Wildtype and mutant crosses on V8 mating media. All images taken at 0.63x magnification scale bar represents 1 mm. B) Quantification of hyphal area for all crosses at all time points. One-way ANOVA with a Dunnet's multiple comparison test of WT hyphal area compared to all mutant crosses * p=0.0366, ** p=0.0033. n=3 biological replicates for all timepoints of hyphal area.

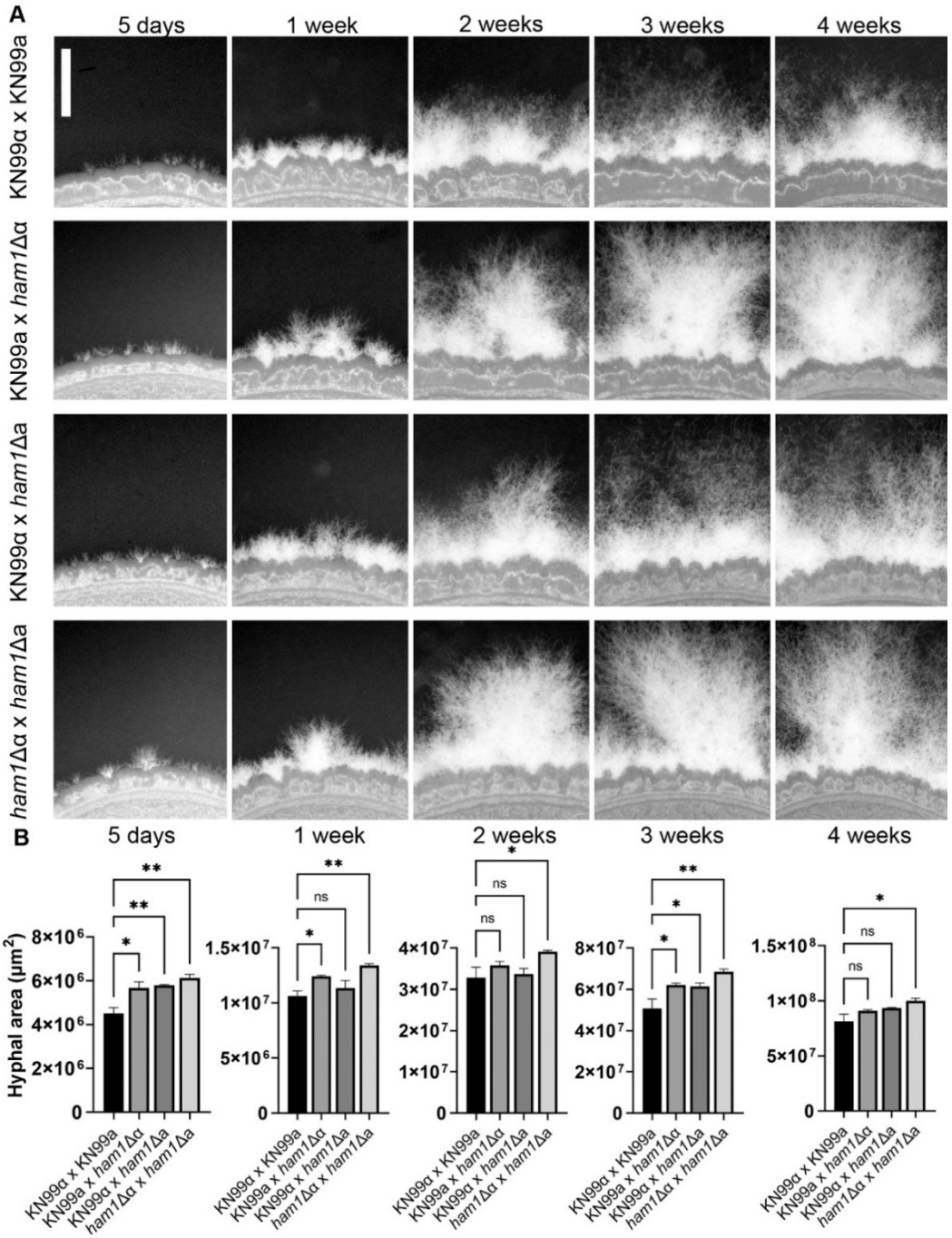
A
5 days
1 week
2 weeks
3 weeks
4 weeks
KN99α x KN99a
KN99a x ham1Δα
KN99α x ham1Δa
ham1Δα x ham1Δa
B
Hyphal area (μm²)
8×10⁶
6×10⁶
4×10⁶
2×10⁶
0
1.5×10⁷
1×10⁷
5×10⁶
4×10⁷
3×10⁷
2×10⁷
1×10⁷
8×10⁷
6×10⁷
4×10⁷
2×10⁷
1.5×10⁸
1×10⁸
5×10⁷
*
**
ns
KN99α x KN99a
KN99a x ham1Δα
KN99α x ham1Δa
ham1Δα x ham1Δa

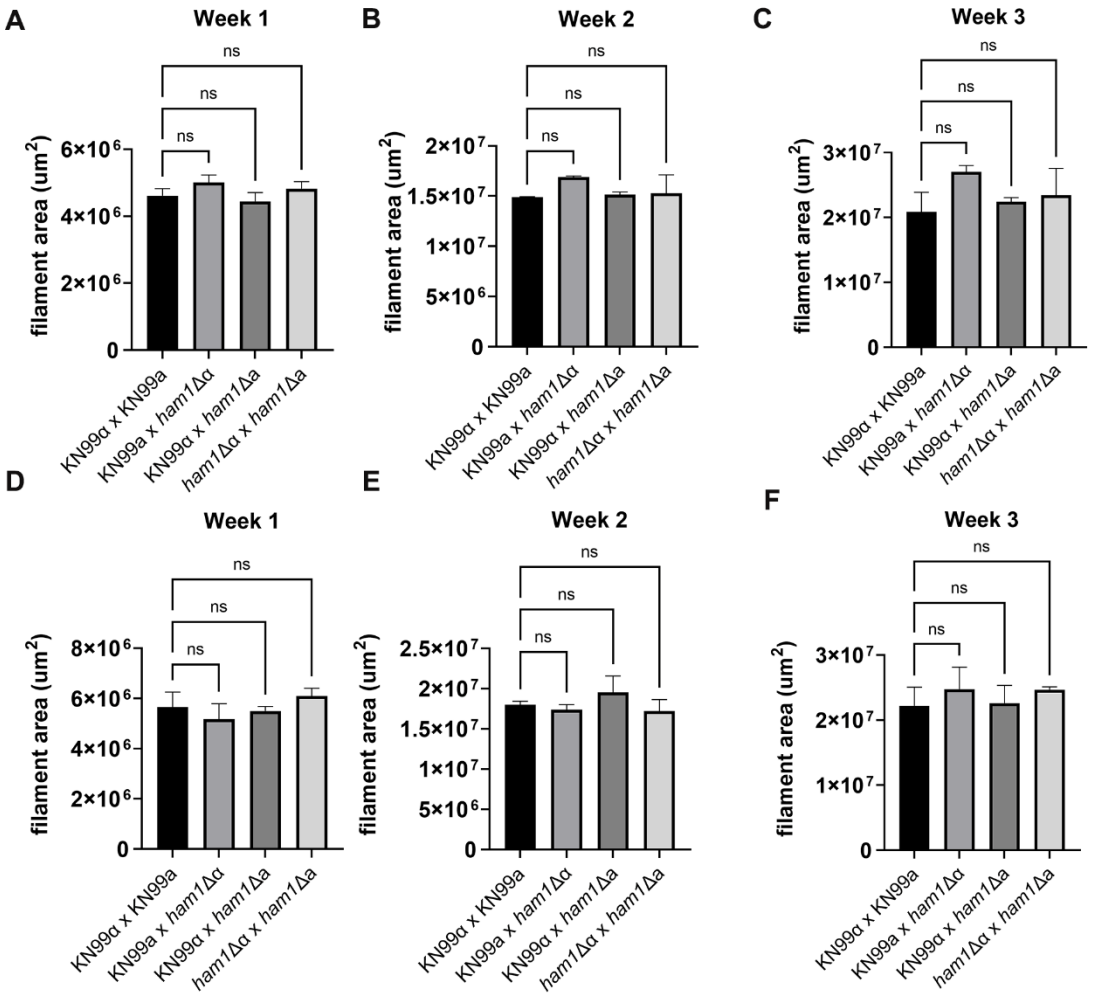

Figure 1.5 *ham1*Δ shows no significant differences in filament area in other mating specific medias. A-C) Filament area of WT and mutant crosses in Murashige-Skoog media a One-way ANOVA with a Dunnet's multiple comparison test of mutants to WT. No significant difference was observed. D-F) Filament area of WT and mutant crosses in Filamentation Agar media a One-way ANOVA with a Dunnet's multiple comparison test of mutants to WT. No significant difference was observed.

2.3.4 *ham1*Δα strain exhibits a fitness disadvantage in both mating and non-mating scenarios.

Mating is an energy costly process, and may result in a fitness cost when comparing mating and non-mating conditions. However, this is crucial for survival in the environment where mating partners are few and far between and the pressures of predators and other stressors threaten survival. We wondered if our *ham1*Δ would display increased fitness compared to a WT competitor due to its propensity to form more hyphae and increased cellular fusion events.

To test this, we had two MATα or two MATa strains with opposing resistance cassettes (the competitors) co-incubated with the opposing mating type with no resistance cassette (the donor) (Fig. 1.6A). All three strains were plated under mating (V8) or non-mating (YPD) conditions for 10 days. At which point, each competitive scenario was scraped, resuspended, and plated on selective media to determine the colony forming units (CFUs) of each competitor (Fig. 1.6A). In the mating permissive condition (V8) we expect both competitors to stop vegetative budding and forage for mating partners, whereas in the non-mating condition (YPD) we expect both competitors to simply divide.

In the WT cross we observed no difference in competitive fitness in either YPD or V8 media conditions, as expected (Fig. 1.6B). However, in our *ham1*Δα competition we saw a dramatic reduction in the competitive fitness of the *ham1*Δα in both the V8 and YPD conditions (Fig. 1.6C). Surprisingly, in our *ham1*Δa competition we observed opposite results, a slight competitive advantage in YPD and no competitive difference in V8 (Fig. 1.6D).

Figure 1.6 *ham1*Δα has a reduced competitive fitness when compared to Wildtype. A) schematic of how cellular competition assay was performed. B) Wildtype competitive fitness presented as a percentage for each cross in either YPD or V8 medium. One-way ANOVA with a Dunnet's multiple comparison test of KN99α NAT initial with YPD and V8 10-day percentages. C) ham1Δα competitive fitness presented as a percentage for each cross in either YPD or V8 medium. One-way ANOVA with a Dunnet's multiple comparison test of ham1Δα NAT initial with YPD and V8 10-day percentages **** $p<0.0001$. D) ham1Δa competitive fitness presented as a percentage for each cross in either YPD or V8 medium. One-way ANOVA with a Dunnet's multiple comparison test of ham1Δa NAT initial with YPD and V8 10-day percentages * $p=0.0238$. n=4 biological replicates for all competition assays.

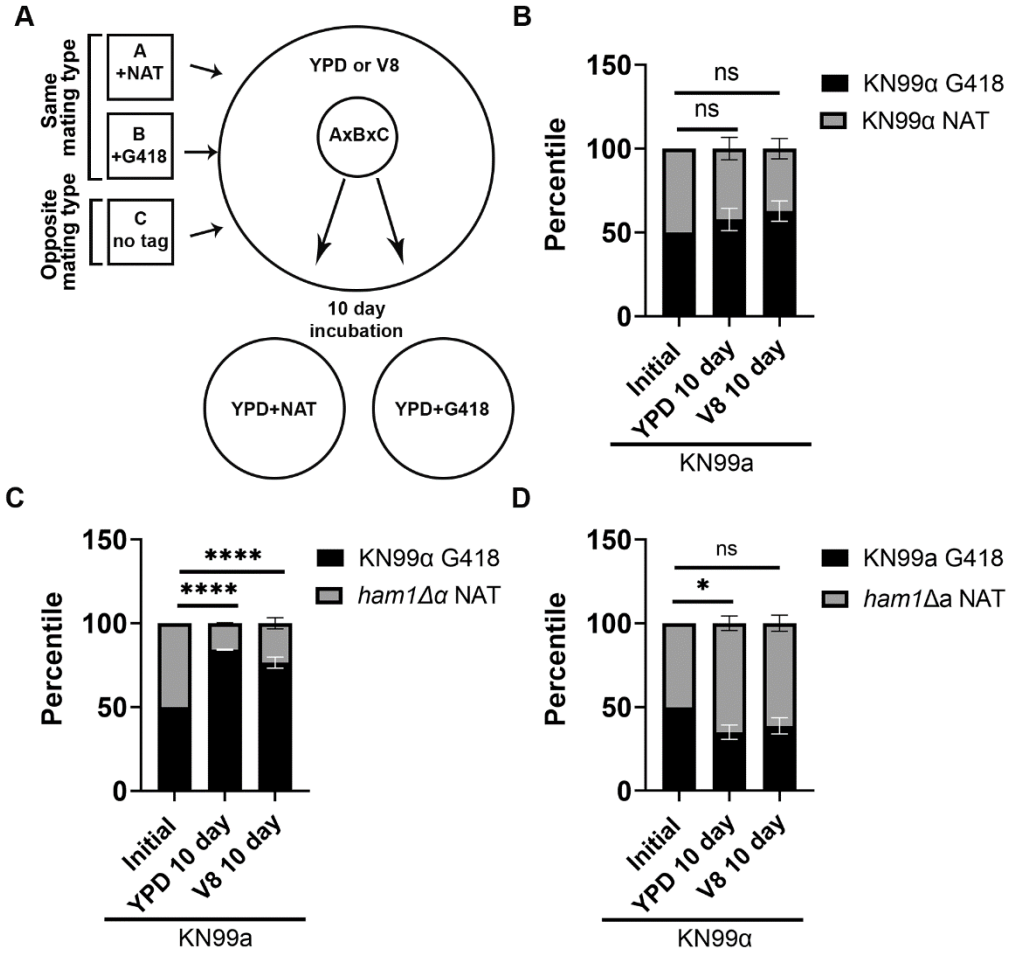
A
Same mating type
Opposite mating type
A +NAT
B +G418
C no tag
YPD or V8
AxBxC
10 day incubation
YPD+NAT
YPD+G418
B
Percentile
150
100
50
0
ns
ns
KN99α G418
KN99α NAT
Initial
YPD 10 day
V8 10 day
KN99a
C
Percentile
150
100
50
0
****
****
KN99α G418
ham1Δα NAT
Initial
YPD 10 day
V8 10 day
KN99a
D
Percentile
150
100
50
0
ns
*
KN99a G418
ham1Δa NAT
Initial
YPD 10 day
V8 10 day
KN99α

2.3.5 Transcriptional analysis of MATα, MATa and *HAM1* over time.

To determine if *HAM1* is involved in the pheromone response MAP kinase pathway, we analyzed the transcriptional activity of the MATα/MATa pheromone loci and *HAM1* under YPD and V8. This type of analyses is typically done in *C. deneoformans*, but when we deleted *HAM1* in this species, mating was unaffected. Since it is known that there are differences in mating regulation between the two sister species, we decided to continue and analyze the transcription of these genes in *C. neoformans*. To do this for the pheromone loci, we compared the gene expression of MATα and MATa in mating conditions normalized to the expression in non-mating conditions to get the relative fold induction (Son et al., 2019, Viviani et al., 2001).

We performed this in a time course of 1, 3, 5 and 7 days to look at changes in expression over time (Fig. 1.7 A-C). While we observed no statistically significant differences in pheromone expression in either MATα or MATa, we saw that the *ham1*Δα unilateral cross trends towards higher MATα pheromone expression at days 1, 3 and 5 and returns to WT levels at day 7 (Fig 1.7 A). For *HAM1* we looked at fold induction in non-mating and mating conditions to see how transcription changed over time. We saw that at day 1 in non-mating conditions *HAM1* had a much higher expression as compared to mating conditions (Fig. 1.7 C). However, as the mating cycle progressed, we observed higher expression of *HAM1* in mating conditions relative to non-mating conditions at days 3 and 5 with a final leveling off in both conditions by day 7 (Fig. 1.7 C). These findings suggest that *HAM1* may be acting as an early mating cycle checkpoint.

Figure 1.7 *ham1*Δ exhibits similar expression of pheromone genes in mating inducing conditions over time. A) Relative transcriptional analysis of MATα (V8 media) conditions relative to non-mating conditions (YPD media) after incubation for 1, 3, 5, and 7 days on respective medias. B) Relative transcriptional analysis of MATa in mating (V8 media) conditions relative to non-mating conditions (YPD media) after incubation for 1,3,5 and 7 days on respective medias. C) Quantification of transcript level of Ham1 in mating and non-mating conditions after incubation for 1, 3, 5 and 7 days on respective medias. There is no significant difference between wildtype and mutant expression levels unless otherwise indicated. n=3 biological replicates for all timepoints and conditions.

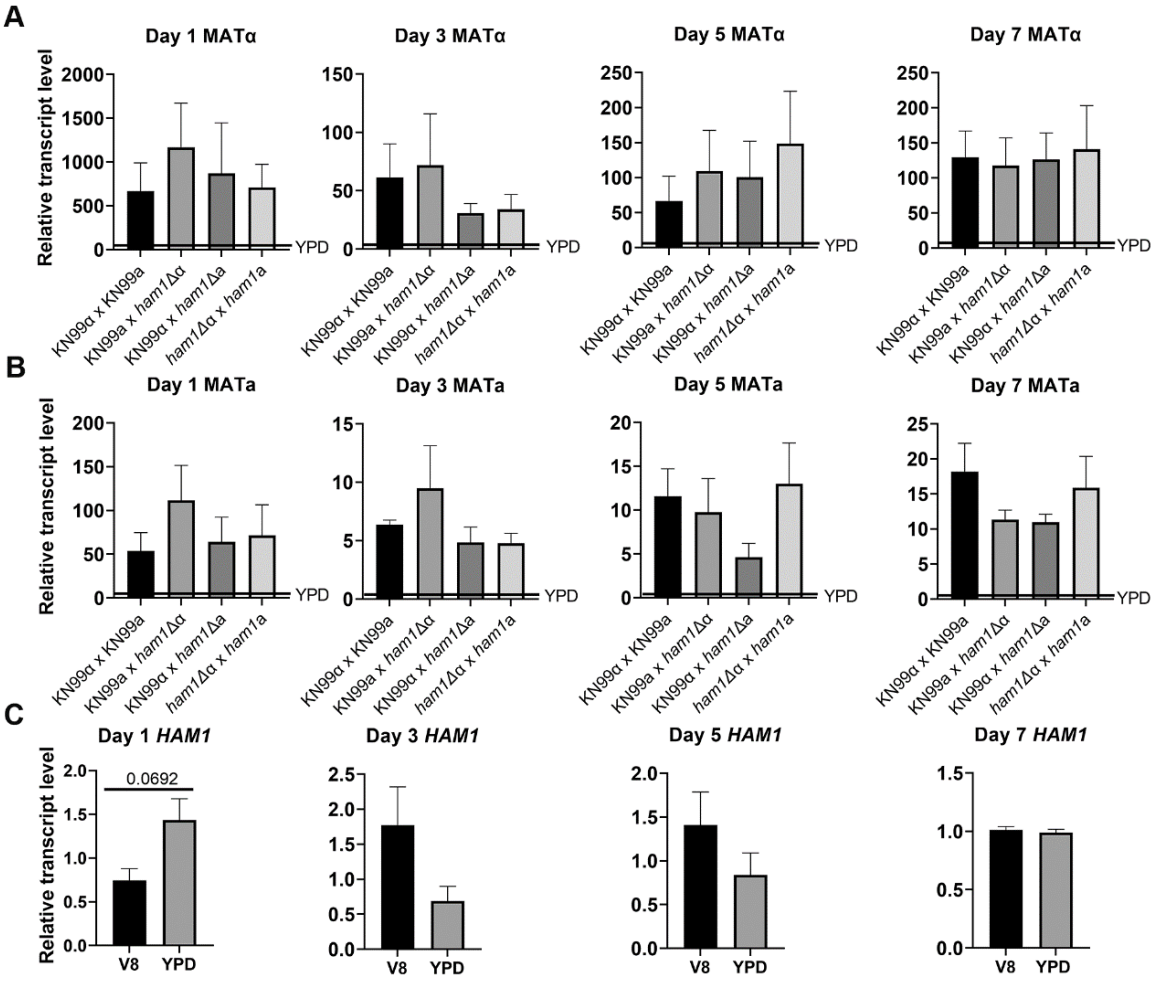
A
Day 1 MATα
Day 3 MATα
Day 5 MATα
Day 7 MATα
Relative transcript level
YPD
KN99α x KN99a
KN99a x ham1Δα
KN99α x ham1Δa
ham1Δα x ham1a
B
Day 1 MATa
Day 3 MATa
Day 5 MATa
Day 7 MATa
C
Day 1 HAM1
Day 3 HAM1
Day 5 HAM1
Day 7 HAM1
0.0692
V8
YPD

2.3.6 Multiple deletion mutants of *ham1*Δ, including a commercial strain (C07), behave similarly in several mating specific assays.

With the recent advances in genetic manipulation and targeted gene deletion methodologies, the Madhani group has been systematically deleting all non-essential genes in the cryptococcal genome (Chun and Madhani, 2010). Using fusion PCR coupled with a biolistic approach, single deletion mutants have been generated through homologous recombination by replacing the gene of interest with a nourseothricin (NAT) resistance cassette (Chun and Madhani, 2010). Our lab acquired the most recent expansion to the original 2015 set which contained a deletion mutant for the *HAM1* coding sequence. We have named this mutant C07 after its well location and have used it in a series of mating assays to validate our phenotypic findings. The entire deletion collection is available commercially (www.fgsc.net).

Consistent with our in house *ham1*Δ mutants, C07 produces abundant hyphae with similar speed and robustness across a 4-week time course (Fig. 1.8 A). When assessing cellular fusion efficiency, we found that our C07 mutant produces abundant double resistant progeny significantly more than our WT cross (Fig 1.8 B).

Figure 1.8 C07 behaves similarly to *ham1*Δ mutants in key mating assays. We tested the C07 mutant (commercial *ham1*Δ) in a variety of assays where we saw phenotypes present in our *ham1*Δ mutants to provide external validation of the phenotypes we were seeing. A) C07 produces hyphae at a similar speed and robustness to our *ham1*Δ mutants. B) C07 produces similar amounts of double resistant progeny to our *ham1*Δ mutants. A One-way ANOVA was run using multiple comparisons to the WT cross ** p=0.0014, ***p=0.0003. n=3 biological replicates for all conditions.

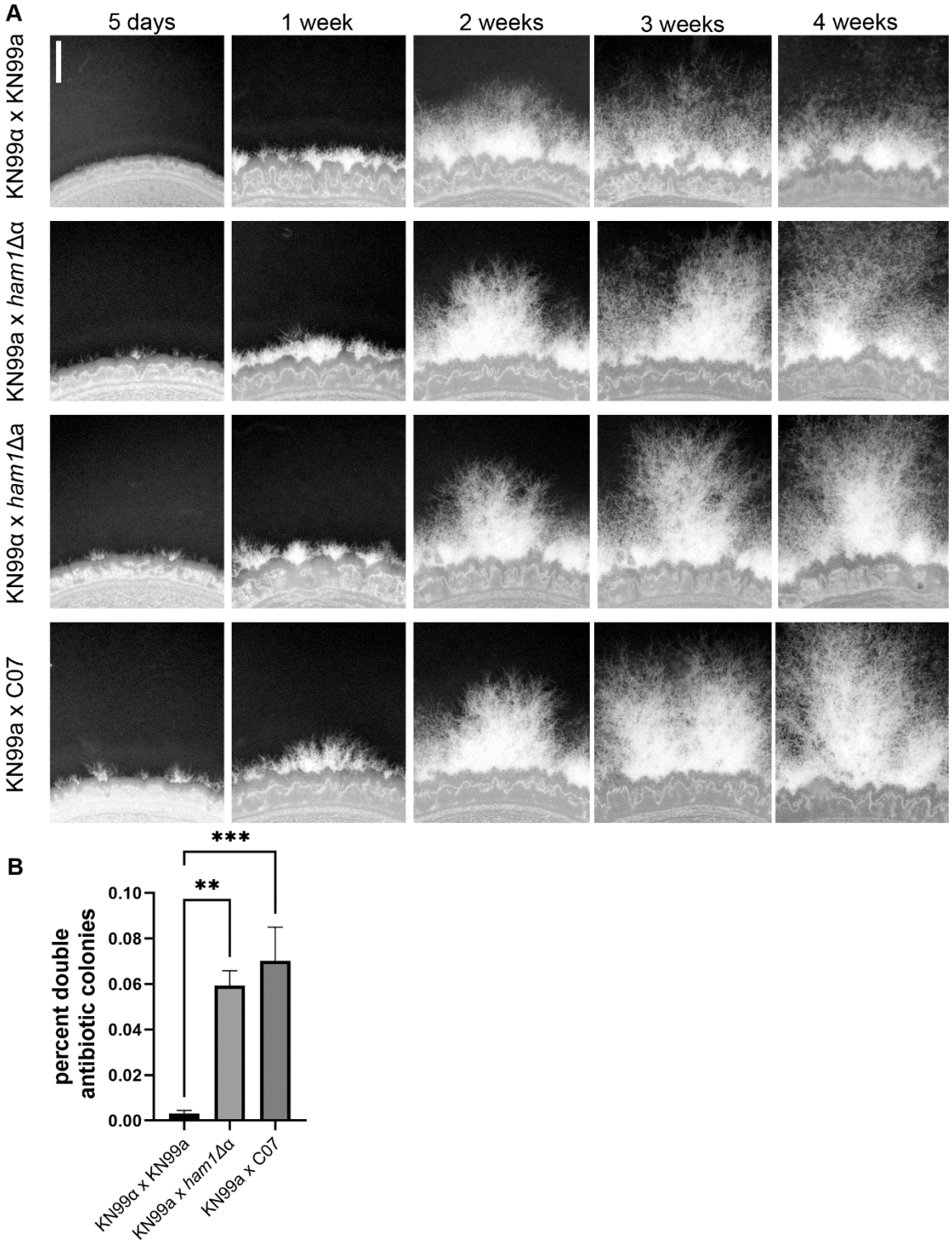
A
5 days
1 week
2 weeks
3 weeks
4 weeks
KN99α x KN99a
KN99a x ham1Δα
KN99α x ham1Δa
KN99a x C07
B
***
**
percent double antibiotic colonies
0.10
0.08
0.06
0.04
0.02
0.00
KN99α x KN99a
KN99a x ham1Δα
KN99a x C07

2.4 Discussion

Mating is a vital part of the lifecycle of *C. neoformans.* It allows for increased genetic diversity among progeny and overall propagation of the species. Despite having a well-defined sexual cycle both in unisexual and bisexual scenarios, not all the important regulators of mating are known, especially in *C. neoformans*. Our results presented here are consistent with *HAM1* acting as a negative regulator of mating specifically in *C. neoformans*.

Understanding mating in *C. neoformans* has been somewhat of a mystery due to the fact that it has never been observed occurring in the environment (Fu et al., 2015) despite indirect evidence that it occurs in Sub-Saharan Africa (Litvintseva et al., 2003). However, under laboratory conditions, mating can be induced very effectively in *C. deneoformans* strain JEC21 (Heitman et al., 1999). Due to its higher propensity to mate bisexually, and its ability to mate unisexually, it has become the standard for understanding mating processes and uncovering the players within these cellular circuits (Wang et al., 2012). Given that mating in *C. neoformans* is not well understood, and considering the larger epidemiological impact of *C. neoformans* over *C. deneoformans*, with *C. neoformans* comprising 95% of clinical isolates and associated with higher virulence potential, we chose to remain in the *C. neoformans* KN99 strain for these mating assessments (Lin, 2008, Barchiesi et al., 2005).

Throughout our mating investigations, we saw the ability of *ham1Δ* mutants to consistently outperform the WT strain in filamentation and production of progeny. This suggests that *HAM1*, like its homolog in *N. crassa*, is somehow connected to the filamentation process in fungal mating and cell-to-cell communication. This was very

apparent in our *ham1Δ* cellular fusion progeny which exhibited a dry desiccated form which were in fact aggregates of hyphae. However, when single colonies of progeny were re-streaked, they returned to a "normal" colony morphology. The presence of the filamentous form in the absence of any mating pressure shows that the progeny of our *ham1*Δ have an even stronger drive towards the mating form but that over time, the signaling to return to a normal yeast state is reestablished.

Additionally, we found the *HAM1* effects were exclusively found in the V8 mating inducing medium as there was no significant increase in the amount of filamentation observed in either MS or FA. V8 media is considered the "gold standard" for looking at mating interactions in *C. neoformans*, while the others are mostly used in *C. deneoformans* (Sun et al., 2019), potentially explaining why we only see phenotypes in V8.

When we investigated competitive fitness, we were surprised to find that our *ham1Δ*α lost in both mating and non-mating conditions whereas our *ham1*Δa had no defects in mating and a slight advantage in non-mating conditions. One of the main differences between cellular competition and other classical mating assays in *C. neoformans*, is that opposite sex mating partners are in very close proximity, which masks issues with searching for mating partners. In our *ham1*Δα competitions we have a few thoughts for why these losses occurred: in the mating permissive scenario *ham1*Δα, while good at making hyphae and producing progeny with a close proximity partner, may lack the ability to forage for mating partners due to a defect in partner seeking. The disadvantage in non-mating permissive conditions may be the result of two possibilities. First, *ham1*Δα has a drive to mate that outweighs the drive to cellularly divide in the presence of an opposite mating partner. Second, in *S. cerevisiae* prolonged exposure to mating pheromones results

in programmed cell death (Severin, et al., 2002). This same principal may apply to *C. neoformans*, with the presence of an opposite mating partner it's possible that the generation of MATα pheromone by our *ham1*Δα may become cytotoxic resulting in either inhibition of cellular growth or death.

Surprisingly, we did not see the same losses in our *ham1*Δa competition. These observations may be the result of the morphological changes occurring on the different mating types. Pre-cellular fusion changes have been observed such as the formation of conjugation tubes reminiscent of *S. cerevisiae* schmooing and the swelling of opposite mating partner cells (Wickes, 2002). To the best of our knowledge, these pre cellular fusion structures have been observed in *C. deneoformans* and are defined by their MAT locus. MATα cells produce conjugation tubes that fuse with swollen MATa cells (McClelland et al., 2004, Kwon-Chung et al., 2014, Fu and Heitman, 2017). If these pre-cellular fusion changes also occur in *C. neoformans* strains, it's possible that in the mating permissive competitive scenario with the *ham1*Δa strain, the WT MATα mating partner is able to produce conjugation tubes to effectively seek the mutant MATa mating partners. These observations, while contrary to what we may have expected given our *ham1*Δα competitive cross, does highlight the possibility that *HAM1* may have a greater effect on MATα strains relative to MATa ones. This finding also highlights the fact that even amongst lab strains there is heterogeneity with respect to competitive fitness and that not all WT strains will behave the same when in a competitive environment, similar to what happens in the environment.

With our findings thus far that *HAM1* is important for proper bisexual mating, we wondered if *HAM1* was acting specifically on the pheromone MAP kinase pathway.

Unfortunately, we were unable to obtain clear results from the qRT-PCR. This was not surprising given that *C. neoformans* strains do not respond to mating signaling uniformly or at the same time, hence the RNA samples represent a mixture of states where mating cells are a minority. Still, we saw a consistent trend where *HAM1* was repressed on V8 early on, as expected if acting as a negative regulator of mating.

Taking a closer look at our MATα and MATa pheromone loci transcription, there appears to be a potential difference in the fold expression of MATα in the *ham1*Δ mutants. While we did not see a significant increase in pheromone transcription, we saw at least a 10-fold increase for all crosses across all time points in the MATα pheromone locus induction relative to the MATa. Our assessment that there may be differences in sensitivity to *HAM1* in MATα vs MATa backgrounds is not a new concept. A previous study looking at the global master regulator *TUP1* and its involvement in mating specific processes found that disruption of *TUP1* led to different gene expression profiles in MATα vs MATa, despite having very similar cellular fusion and filamentation phenotypes (Lee et al., 2005)

One of the hallmarks of mating in *C. neoformans* is the morphological transition from yeast to hyphae. The hyphal form of *C. neoformans* has been shown to be unable to cause disease in a mammalian host in part because it induces an immune response shift from a disease permissive Th-2 to a disease protective Th-1 proinflammatory response. When examining previously published RNA-seq data it was noted that *HAM1* transcripts were some of the highest induced in cryptococcal meningitis patients (Yu et al., 2021, Chen et al., 2014). This finding is intriguing for two reasons. First, it lends support to the idea that to prevent a morphological transition in this low nutrient environment, negative regulators of mating would be highly expressed. Secondly, it may indicate additional roles

for *HAM1* directly related to maintenance of virulence factors providing further evidence of the link between mating and virulence. By studying mating, we not only gain a greater understanding of this essential biological process but also an appreciation at the intricacy of how this pathogen is able to survive and propagate in the environment despite the numerous predative pressures it faces.

2.5 Methods

2.5.1 Strains and Growth materials

All strains were in the KN99 background (Nielsen et al., 2003). All *ham1*Δ strains and Ham1-FLAG tagged strain were generated using biolistic delivery (see methods below). V8 agar medium was generated using original recipe V8 juice, bacteriological grade agar and dH20. V8 medium was adjusted to the appropriate pH (5 for *C. neoformans*, 7 for *C. deneoformans*) using 1M Hydrochloric Acid or sodium hydroxide tablets, respectively. 25mM $CuSO_4$ was added after autoclaving before pouring plates.

2.5.2 Generation of deletion strains and tagged strains by biolistic and mating methods

We generated all *ham1*Δ mutants using the split marker method to delete the entire *HAM1* coding region. Fragments were delivered to candidate KN99α and KN99a cultures via biolistic delivery (Bio-Rad PDS-1000). Deletion candidates (at least two independent colonies) were assessed using PCR as well as mating phenotype analysis to confirm deletions. To perform immunoprecipitations needed for the click chemistry analyses, a FLAG-tagged strain was generated using the 4x FLAG-Tag plasmid (Jung et al., 2018) to tag the C-terminal end of Ham1. This fragment with overlapping homology to the *HAM1* coding sequence was synthesized by Genewiz and again delivered into both KN99α and KN99a via biolistic delivery. We were able to only successfully obtain a FLAG-tagged strain in our KN99a background.

In addition to generating deletion mutants via biolistics, we also generated two independent *ham1*Δa candidates via mating of WT with *ham1*Δα. Strains were grown in 5

mL of YPD for 48 hours, spun down and washed twice in dH20, counted, and normalized to a concentration of 1.5 x10^7 cells/mL. Equal cell volumes of each mating pairs were mixed and incubated at RT for an hour. 100-200 uL of this mixture was spotted onto V8 mating plates and incubated in the dark at RT for 7 days. Spores from mating interaction were scraped using a sterile toothpick and resuspended in dH20. Spores were plated on YPD with selection agar plates and streaked twice with selection for single colonies. Isolated single colonies were tested for mating type using a mating interaction with known tester strains (JEC20 and JEC21).

2.5.3 Cell preparation and protein extraction of palmitate fed cells

HAM1-FLAG tagged strains and KN99a strains were grown in 50 mL of YNB medium, pH 7.0. Once an OD of 0.5 was reached, strains were fed with 15uL of 5uM Alkynyl Palmitic Acid (Click Chemistry Tools #1165) and incubated for 1hr at 30°C with shaking. Cells were washed twice in cold dH_20 and flash frozen until ready for use. Cells were thawed on ice and disrupted in lysis buffer (100 mM Tris-HCl pH 7.4, 0.5% Triton X-100, 150mM NaCl, 13% w/v glycerol, protease inhibitor tablet, Roche) by bead beating (mini bead beater-16, #607) for 5 cycles 1 minute on 1 minute rest on ice. Cell extracts were spun down at 13,000 x g for 10 minutes at 4C. Protein concentration of the supernatant was determined by a detergent compatible Bradford assay (Thermo-Scientific #23246).

2.5.3.1 Immunoprecipitation and Click Chemistry

Based on the methods described in Yount et al., 2011, 1 ug of protein lysates from fed and unfed cell populations were incubated with 100 uL of 50% slurry of anti-FLAG M2 affinity gel (A2220; Sigma-Aldrich) for 20 minutes on a nutator at 4C. The protein-

bead mixtures were then loaded onto a gravity column (TALON 2 mL Disposable Gravity Column, Takara #635606). Lysate was loaded into the column 5 times with gravity flow and then washed in a 1M NaCl buffer 3 times. Beads were then washed twice in a 150mM salt buffer to prevent issues with downstream SDS-PAGE. Click Chemistry reaction was done according to manufacturer's protocol (#1262, Click Chemistry Tools) apart from the AFDye 680 Azide Plus reporter which was added at a concentration of 1.25uM as opposed to the recommended 40uM (Click Chemistry Tools #1512).

Excess reactants were removed by spinning down anti-FLAG M2 affinity gel and washing twice in 1x PBS. Beads were then resuspended in 1x Laemmli Buffer and heated at 70°C for 10 minutes. After SDS-PAGE the 10% polyacrylamide gel was destained in Click Chemistry Destain (40% (v/v) methanol 50% (v/v) acetic acid 10% (v/v) water) overnight and gel visualized on an Odyssey Imaging System (LI-COR Biosciences).

2.5.4 Cellular Fusion

Cellular fusion efficiency was assessed using overnight cultures grown in YPD that were washed twice in dH20. Cultures were normalized to an OD of 0.5 and resuspended in dH20. Each cross is comprised of cells of opposite mating type and different antibiotic resistance cassettes to determine the fusion efficiency of each cross. Equal volumes of each strain are mixed for their respective crosses and spotted in 50uL increments on V8 mating agar. Each cross is spotted in triplicate and left to dry for 20 minutes.

Once all plates were dry, they were transferred to a mating chamber (DM1, Mycolabs) and left in the dark for 5 days at ambient room temperature with a relative humidity of 40-50%. After incubation, each cross was scraped and resuspended in 1 mL of

dH20 and normalized via cell count to $1x10^7$ cells/mL. For quantification, 100 uL of undiluted, or 10 and 100-fold dilutions of the $1x10^7$ cells/mL suspension, was plated on both double and single antibiotic YPD resistance plates (NAT and NEO). Once plates were dry, they were transferred to a 30°C room, incubated for three to four days, and counted for CFUs.

2.5.5 Cellular Fusion with synthetic exogenous pheromone

The MFα1 sequence for synthesis was obtained from Fu et al., 2019 and synthesized by GenScript. Upon receipt lyophilized synthetic pheromone was resuspended in 100% Methanol. Working stocks were generated at a concentration of 50 µM and added to bisexual mating crosses at final concentrations of 5-10 µM. Exogenous pheromone was added to 200ul of pre-mixed bisexual crosses before being plated on V8 medium.

2.5.6 Hyphal staining and visualization

Single colonies from mutant crosses were scraped and resuspended in dH20. Colonies were then stained with either 5 ug/mL DAPI or 100 ug/mL Calcofluor White (CFW) and incubated at 30°C in the dark for 20 minutes. Cells were then washed three times in 1x PBS and resuspended in 100 uL. Cells were then imaged using a 100x oil immersion objective in a Zeiss Axio Observer microscope.

2.5.7 Assessment of Bisexual mating

Adapted from Bisexual Mating Protocol from Sun et al., 2019. Briefly, strains were grown overnight in YPD, washed twice in dH20 and normalized to an OD of 1. Cells of

opposite mating type for each cross were mixed in equal amounts in a separate tube and subsequently spotted in 20 uL amounts onto V8 agar plates. All crosses were spotted in triplicate and left to dry for 20 minutes. Once all plates were dry, they were transferred to a mating chamber (DM1, Mycolabs) and left in the dark for 3-4 weeks with a relative humidity of 40-50%.

2.5.8 Cellular Competition assessment

Each cross consists of three strains: two of the same mating type and opposing antibiotic resistance cassettes (competitor strains) and one of the opposite mating type with no antibiotic resistance (donor strain). Overnight cultures for each strain were grown in YPD and adjusted to log phase. Cultures were then washed twice in dH20, counted, and normalized to a concentration of $1x10^5$ cells/ml. Competitor and recipient strains were mixed in equal amounts for each cross. 30 uL of each cross was plated in triplicate on V8 and YPD medium and left to dry for 20 minutes. Once all plates were dry, they were transferred to a mating chamber and left in the dark for 10 days with a relative humidity of 40-50% After the 10 days crosses were scraped and resuspended in dH20. Crosses in YPD were diluted 100,000x and crosses in V8 were diluted 10,000x. 100 uL of the respective dilutions was plated single antibiotic supplemented YPD plates (NAT or G418). Plates were incubated for 2-3 days and imaged for CFUs using a Bio-Rad Gel Doc EZ imager.

2.5.9 RNA isolation and RT-qPCR from bisexual mating crosses

Bisexual mating crosses are set up as previously described and allowed to incubate for 1, 3, 5 and 7 days. Cells are then harvested, washed once in dH20, washed with RNA stop solution and flash frozen and stored at -80°C until ready for extraction. A TRIzol-

extraction (Life Technologies #15596-026) protocol is used followed by an RNA clean up step using the ZYMO RNA Clean and Concentrator kit (cat # R1019). Up to 1ug of RNA is then converted into cDNA using the NEB LunaScript® RT Supermix Kit (NEB #E3010) followed by qPCR using the NEB Luna Universal qPCR Master Mix (NEB #M3003). The $\Delta\Delta_{CT}$ method was used for quantification of relative transcript level normalized to YPD samples (Livak and Schmidttgen 2001).

CHAPTER 3:

ABSENCE OF *HAM1* AFFECTS SEVERAL VIRULENCE TRAITS

3.1 Abstract[2]

Our initial studies on *ham1*Δ showed that the mutant seems to be more prone to enter the mating process even under non-mating conditions. Consistently, *ham1*Δα has a competitive fitness defect under both mating and non-mating conditions. Previous reports have linked changes in mating to altered virulence capacity, hence, we wanted to investigate if *ham1*Δ exhibited any differences in virulence factors or virulence capacity.

We found several differences with the major virulence factor, the polysaccharide capsule. We found that our *ham1*Δ has defective capsular retention, is less effective at donating its capsule to acapsular strains, shows increased exopolysaccharide shedding under certain conditions, and has a significant increase in biofilm formation relative to WT. Surprisingly, when tested *in vivo* using the invertebrate model *Galleria mellonella*, we found no major defects in virulence and no difference in fungal burden of *ham1*Δ mutants relative to WT. Still, understanding the connection between mating and virulence through the study of *HAM1* dysfunction may open new avenues of investigation into ways to improve the treatment of this disease.

---

[2] This chapter contains work that is currently under review at Microbiology Spectrum. To access the preprint please see this citation: Yee, E. A., Ross, R. L., & Santiago-Tirado, F. H. (2023). Phenotypic characterization of *HAM1*, a novel mating regulator of the fungal pathogen *Cryptococcus neoformans*. *bioRxiv*, 2023.2009.2018.558251. https://doi.org/10.1101/2023.09.18.558251

3.2 Introduction

Several studies have shown an inverse relationship between *C. neoformans's* virulence and its filamentous mating form (Lin 2009). For example, when *ZNF2,* a master regulator of filamentation in *C. neoformans*, is constitutively overexpressed, the cells are morphologically hyphal-locked and unable to cause disease in a mouse model (Wang et al., 2012). These hyphal-locked cells induced a protective Th1 pro-inflammatory immune response that not only resulted in full control of the initial infection, but also in protection from subsequent challenges, and hence has been implicated as a successful vaccination strategy in mouse models that are immunocompetent and immunocompromised (Zhai et al., 2015, Pham et al, 2023). This suggests that mating regulators may also play a larger role in control of virulence mechanisms, such as impacting any one of the main cryptococcal virulence factors: the polysaccharide capsule, growth at human body temperature, and melanization. While each of these virulence mechanisms has been comprehensively studied, not all the mating regulators have been uncovered, especially in *C. neoformans* (as opposed to *C. deneoformans*).

We have shown *HAM1* has a role in the mating cycle of *C. neoformans* but we did not know if there were additional impacts on virulence or virulence factor production. Although we do not observe major defects in capsule generation and other key virulence mechanisms, we found that our *ham1*Δ strains in the MATα background exhibited defects in capsule attachment, an increase in capsule shedding, less effective capsule transfer, and an increase in biofilm production. These alterations in *ham1*Δ mutants can potentially affect their virulence, however, surprisingly, when we infected the invertebrate waxworm *Galleria mellonella* we observed no difference in survival or fungal burden relative to WT.

Still, our findings suggest a connection between mating and proper capsule formation and shedding, further proving that mating and virulence pathways are interconnected in this fungal pathogen.

3.3 Results

3.3.1 *ham1*Δ mutants show no defects in major virulence factors.

So far, all the phenotypes of the *ham1*Δ have been mating related, especially in the MATα background. We wondered if these would also affect virulence, hence we investigated if our *ham1*Δ mutants (in both MAT backgrounds) had defects in the main virulence factors of *C. neoformans*: capsule production, ability to melanize, thermotolerance (growth at 37°C), and recognition by phagocytic cells (Fig. 2.1). We found no obvious differences in any of the major virulence mechanisms (Fig. 2.1).

Figure 2.1 *ham1*Δ shows no defects in major virulence mechanisms. A) Representative images of induced capsule stained with India Ink. Scale bar represents 10um. B) Measurement of capsule radius after induction, n=20 cells for all strains. C) Melanin induced on caffeic acid plates; *lac1*Δ is a melanin mutant and serves as a negative control. D) Measurement of uptake by THP-1 phagocytic cells as a function of the number of engulfed fungi divided by the number of THP-1 cells, normalized to the WT condition; *pbx1*Δ is a known mutant with a higher uptake index and *opt1*Δ is a known low uptake index. A One-way ANOVA test was run on all strains with the MATα background, this includes our positive (*pbx1*Δ) and negative (*opt1*Δ) controls using a Dunnet's multiple comparison test to KN99α * $p=0.256$, **** $p<0.0001$. A Student's t-test using a Gaussian distribution was used to compare phagocytic indices of KN99a and *ham1*Δa as they are both the MATa background.

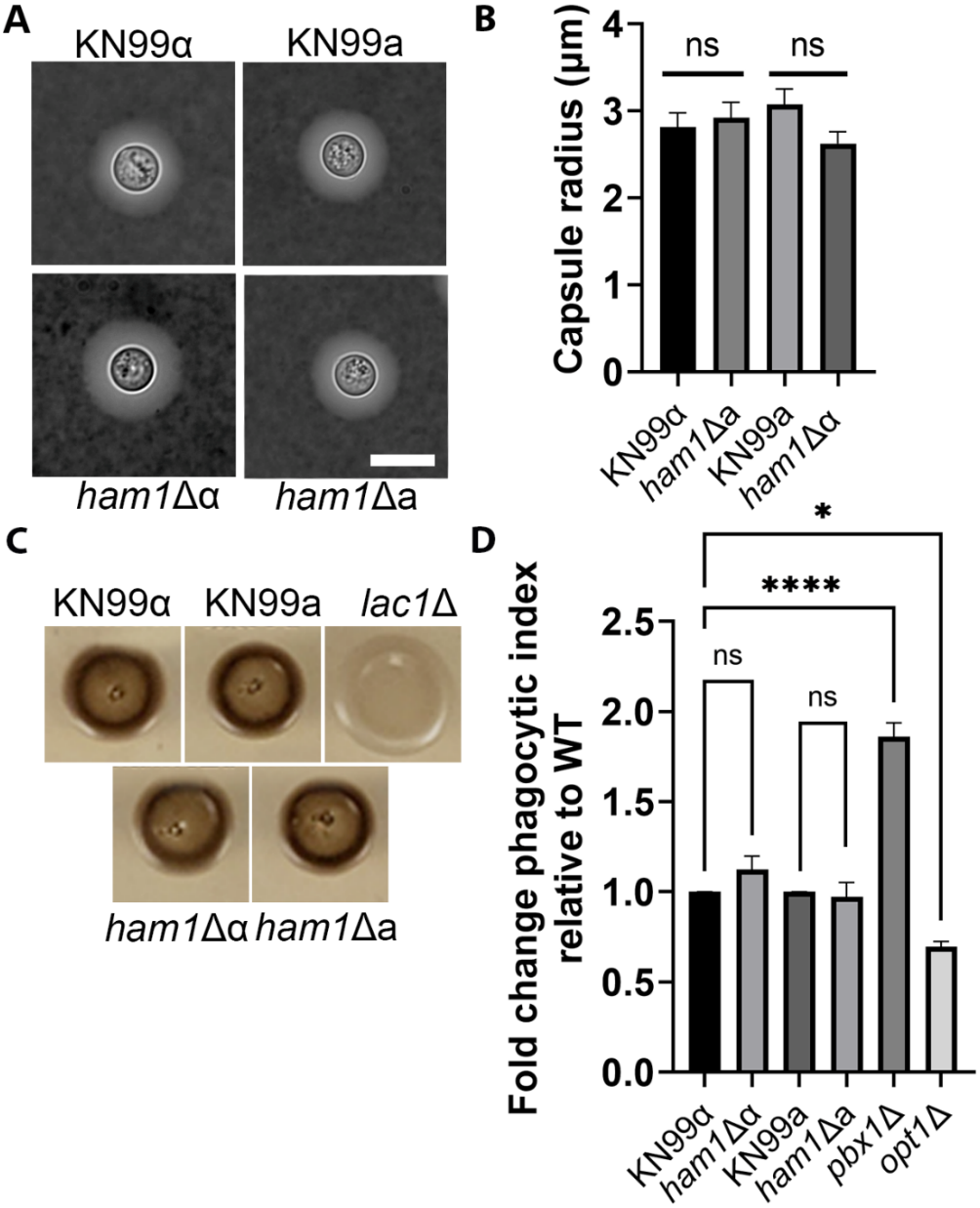
A
KN99α
KN99a
ham1Δα
ham1Δa
B
Capsule radius (μm)
ns
ns
KN99α
ham1Δa
KN99a
ham1Δα
C
KN99α
KN99a
lac1Δ
ham1Δα
ham1Δa
D
Fold change phagocytic index relative to WT
*
****
ns
ns
KN99α
ham1Δα
KN99a
ham1Δa
pbx1Δ
opt1Δ

3.3.2 *ham1*Δ mutants show no sensitivities to various cell wall, cell membrane and antifungal stressors.

Due to the surface defects observed in the *pfa4*Δ we wanted to take a closer look at the cell wall and cell membrane of our *ham1*Δ strains. As a downstream target of Pfa4, it is possible that there may be more nuanced differences with either the cell wall or capsule besides induction. We subjected our *ham1*Δ strains to a variety of cell wall, membrane and antifungal stressors on solid agar plates (Fig. 2.2). Finding no apparent defects under any of the different cell wall and membrane stressors or antifungal stressors we tested, we took a closer look at the polysaccharide capsule and investigated differences in its attachment and release.

Figure 2.2: *ham1*Δ shows no sensitivities to various cell wall and membrane stressors as well as antifungal treatments. As part of our initial survey for defects in our *ham1*Δ mutants we wanted to test some standard cell wall and membrane stressors. A) To rule out any issues with calcineurin signaling we tested various calcium concentrations in YPD solid agar medium. We also wanted to test any issues with the cell membrane by using various concentrations of sodium dodecyl sulfate (SDS); no sensitivities were observed in any of these plates. B) Next, we tested thermal stress (YPD at 30 and 37C), osmotic stress (NaCl), Nutrient stress (YNB), and cell wall stress signaling (Caffeine); no sensitivities were observed under any of these conditions at 30 or 37C. C) Next, we tested cell wall stress (Calcofluor white, CFW), Oxidative stress (H2O2) and Oxidative stress (NaNO3); no sensitivities were observed under any of these conditions. D) Finally, we tested sensitivity to common antifungals Amphotericin B and Fluconazole; no sensitivities were observed in either antifungal

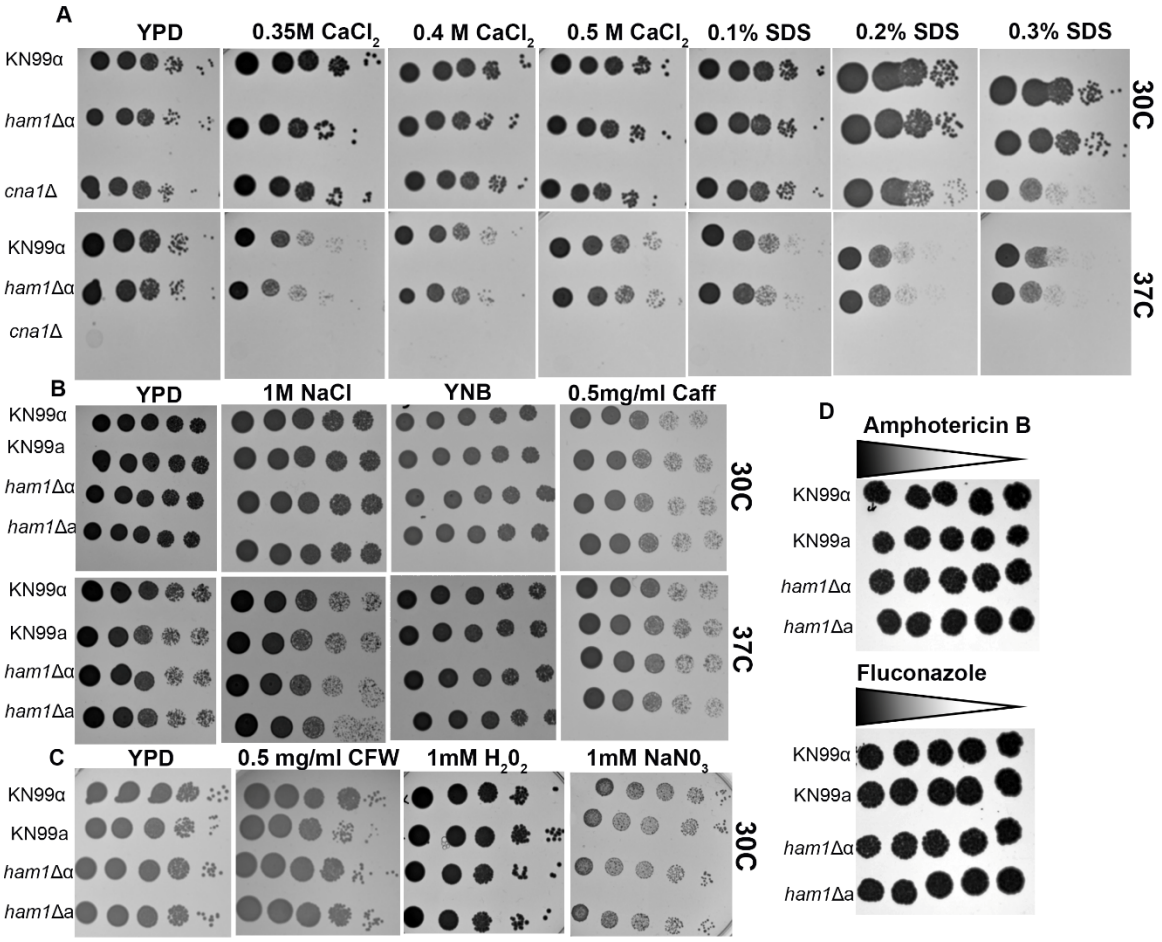
A
YPD
0.35M CaCl2
0.4 M CaCl2
0.5 M CaCl2
0.1% SDS
0.2% SDS
0.3% SDS
KN99α
ham1Δα
cna1Δ
30C
37C
B
YPD
1M NaCl
YNB
0.5mg/ml Caff
KN99a
ham1Δa
C
0.5 mg/ml CFW
1mM H2O2
1mM NaNO3
D
Amphotericin B
Fluconazole

3.3.3 *ham1Δ*α exhibits defects in capsule attachment and transfer.

For these assays we focused on our *ham1*Δ deletions in the MATα background since our major mating phenotypes were more predominant in MATα, and because of the epidemiological factor that the majority of clinical isolates are MATα. First, we looked at capsule attachment. After inducing capsule formation, we subjected WT, *ham1*Δα and a known capsule mutant (*pbx1*Δ) to sonication, and then measured the capsule size pre- and post-sonication (Fig. 2.3 A). We found that our *ham1*Δα mutant lost significantly more capsule than WT cells, suggesting a defective attachment to the cell wall (Fig. 2.3 B, Fig. 2.6).

Given the defective attachment, we next investigated capsule transfer from a donor cell to an acceptor acapsular cell. We incubated the acapsular mutant *cap59*Δ with conditioned media from WT, *ham1*Δα, *pbx1*Δ and *cap59*Δ to see how well the shed capsular material could attach to the cell wall of *cap59*Δ (Fig. 2.3C). As expected, our *cap59*Δ mutant could not transfer capsule at any dilution tested due to the lack of capsule in this mutant. Our *pbx1*Δ mutant also was unable to transfer capsule at dilutions higher than 1:5 which was unsurprising due to its known capsule defects (Liu et al., 2007, Kumar et al., 2014). However, our *ham1*Δα also struggled to transfer the capsule at higher dilutions >1:750, whereas the WT capsule had no problem at these dilutions. This indicates at least a small defect in either structure or reduced release of capsule (Fig. 2.3 C, Fig 2.6). Defects indicated by sonication and transfer in our *ham1*Δα prompted us to look at shedding and

biofilm production which could further confirm issues with capsular release (Denham et al., 2018)

Figure 2.3 *ham1*Δα exhibits defects in capsule attachment and transfer. A) Representative images of wildtype, *ham1*Δα and *pbx1*Δ capsules stained in India Ink before and after sonication. Scale bar represents 5um. B) Quantification of the percentage of capsule retained post sonication. One-way ANOVA with a Dunnet's multiple comparison test to WT ** p=0.0041, **** p<0.0001 n=20 cells for all strains. C) Representative images of capsule transfer capsule visualized by conjugated 3C2 antibody with Alexa488 fluorescent probe and cell wall stained with Calcofluor white (CFW) scale bar is 10um.

Δ

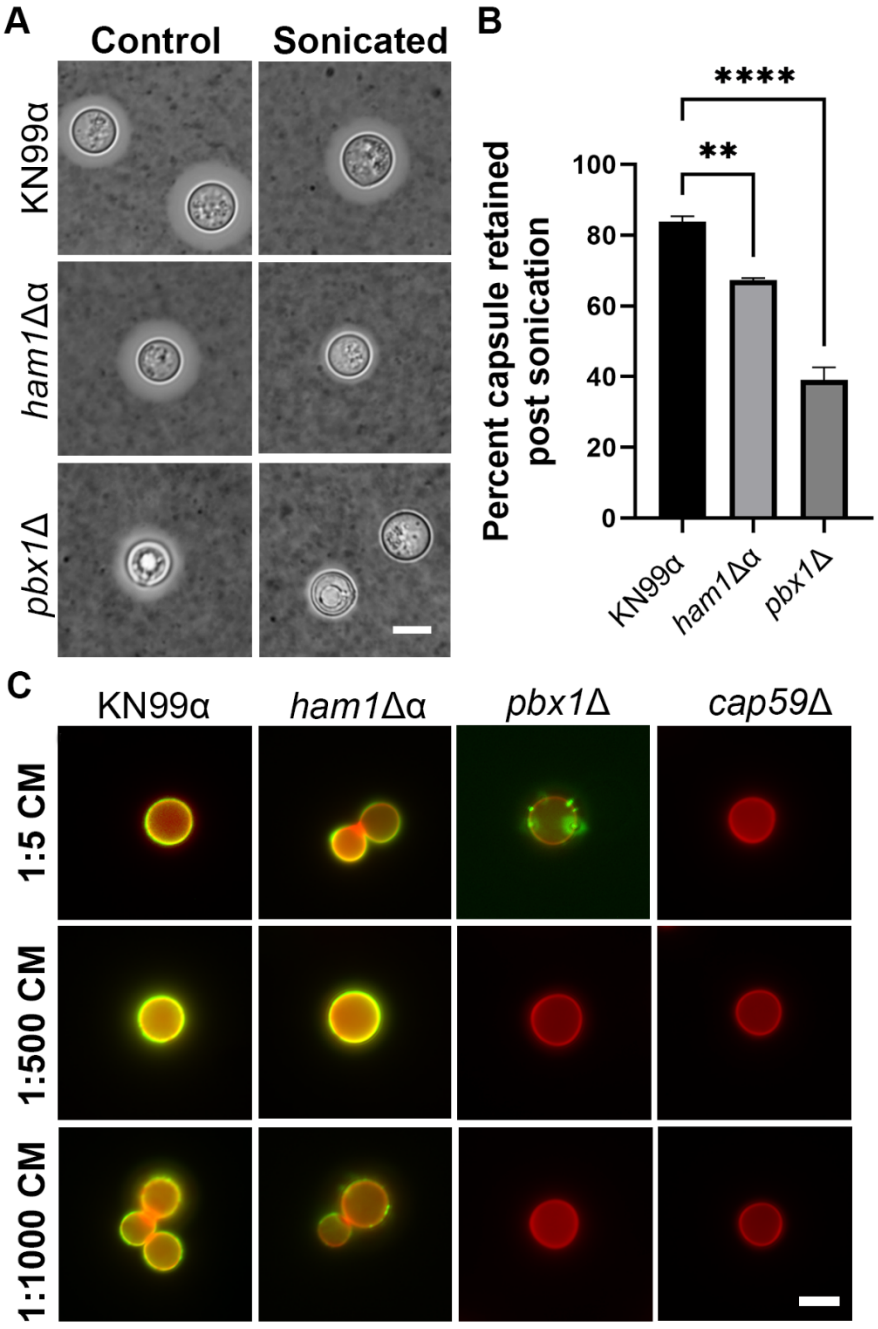
A
Control
Sonicated
KN99α
ham1Δα
pbx1Δ
B
Percent capsule retained post sonication
100
80
60
40
20
0
**
****
KN99α
ham1Δα
pbx1Δ
C
KN99α
ham1Δα
pbx1Δ
cap59Δ
1:5 CM
1:500 CM
1:1000 CM

3.3.4 *ham1*Δα exhibits increased exopolysaccharide shedding in non-capsule inducing media and trends towards more shedding in capsule inducing media.

To investigate the possibility of defects with capsule release, we assessed the ability of *ham1*Δα to shed capsule in different media by electrophoresis and immunoblotting (Yoneda and Doering, 2008 Denham et al., 2018) (Fig. 2.4A). We observed distinct differences in the size of the shed polymer populations in nutrient-rich YPD medium with potential differences in the capsule-inducing medium DMEM and the minimal growth medium YNB (Fig. 2.4A). To get a more quantitative measurement, we measured GXM concentration by ELISA (Denham et al., 2018).

In YPD we saw a significant increase in the amount of capsule shed in our *ham1*Δα (Fig. 2.4B). We saw no significant difference in the amount of capsule material shed in YNB or DMEM relative to WT, although in both there was a trend towards higher capsule shedding in our *ham1*Δα (Fig 2.4 B-D, Fig 2.6). For all media, our capsule shedding mutant *pbx1Δ* shed less than WT, and our acapsular mutant *cap59Δ* did not shed any capsule, as expected (Kumar et al., 2007). Given the association between capsule and biofilm formation, we next assessed how well *ham1*Δα could produce a biofilm using the XTT biofilm assay (Pierce, et al., 2008). We found that our *ham1*Δα, similar to our *pbx1*Δ, produced larger biofilms than our WT strain, whereas no biofilm was produced in the acapsular mutant *cap59*Δ (Fig. 2.4E).

Figure 2.4 *ham1*Δα exhibits increased exopolysaccharide shedding and biofilm production A) Representative GXM immunoblot of exopolysaccharide shedding in capsule non-inducing media YPD and minimal media YNB. B) Representative GXM immunoblot of exopolysaccharide shedding in capsule inducing media DMEM. C) Quantification of shed exopolysaccharide in YPD via sandwich ELISA as fold change relative to WT. A One-way ANOVA with a Dunnet's multiple comparison test of WT to *ham1*Δ and *pbx1*Δ. * p=0.0133, 0.01339 respectively. D) Quantification of shed exopolysaccharide in YPD via sandwich ELISA as fold change relative to wildtype. A One-way ANOVA with a Dunnet's multiple comparison test of WT to *ham1*Δ and *pbx1*Δ. ** p=0.0064. E) Quantification of shed exopolysaccharide in DMEM via sandwich ELISA as fold change relative to wildtype. A One-way ANOVA with a Fisher's LSD test was run on all samples ** p=0.0069. n=3 biological replicates for all ELISAs.

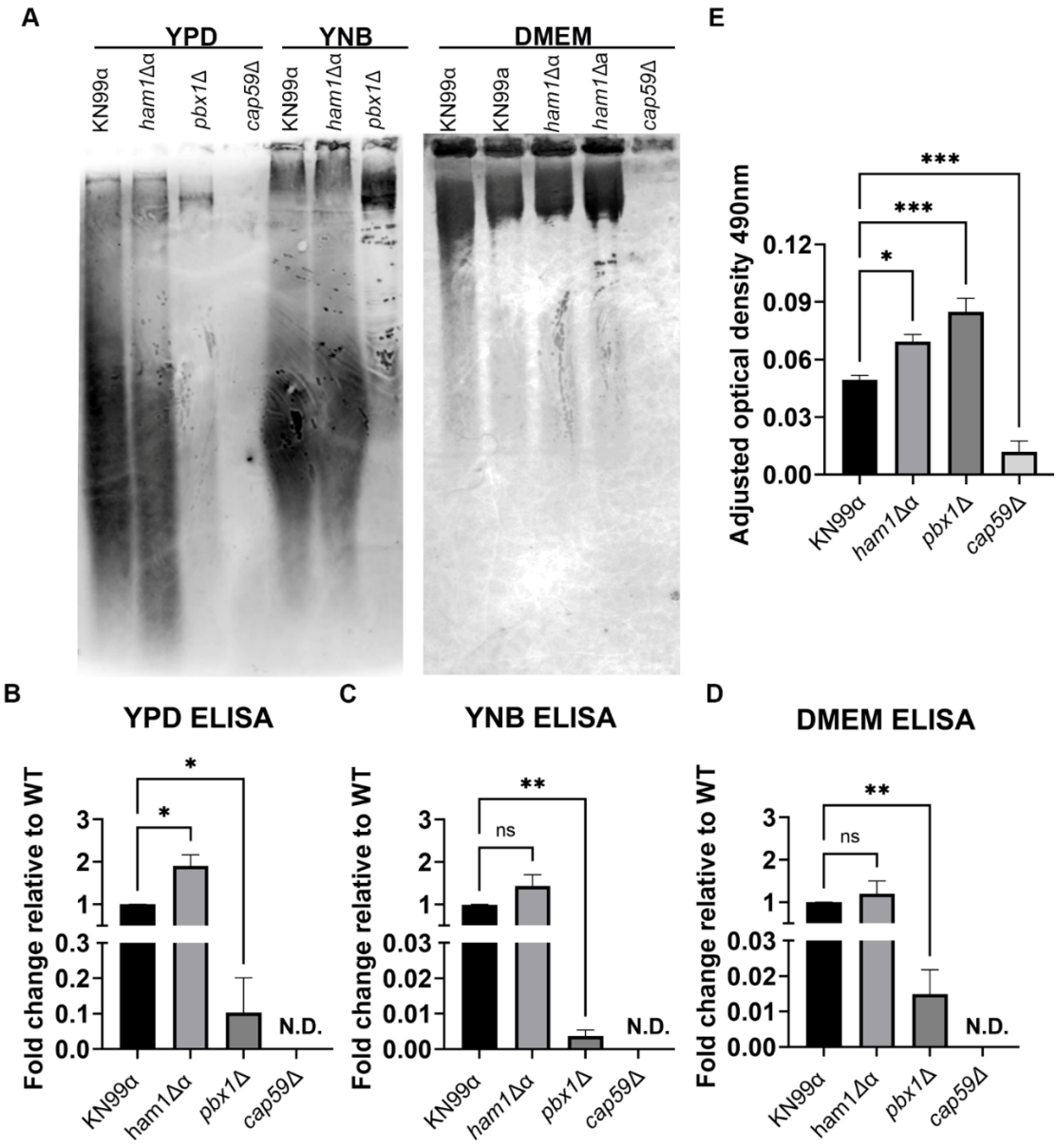
A
YPD
YNB
DMEM
KN99α
ham1Δα
pbx1Δ
cap59Δ
KN99a
E
Adjusted optical density 490nm
B
YPD ELISA
C
YNB ELISA
D
DMEM ELISA
Fold change relative to WT
N.D.
ns

3.3.5 *ham1*Δα shows no difference in virulence capacity in the invertebrate *Galleria mellonella* model.

Lastly, to investigate whether the role of *HAM1* in mating and proper capsule function translates to virulence defects, we performed infections using the invertebrate model system *G. mellonella*. We infected G. *mellonella* larvae with $1x10^5$ log phase cells and, surprisingly, saw no significant difference in survival between WT and independent *ham1*Δα mutants (Fig. 2.5 A, Fig. 2.6). On the other hand, the *pbx1*Δ mutant showed attenuated virulence which is consistent with previous studies (Liu et al., 2007). We also assessed fungal burden at time of death, but saw no significant difference in the fungal burden with any of the strains (Fig. 2.5 B, Fig. 2.6).

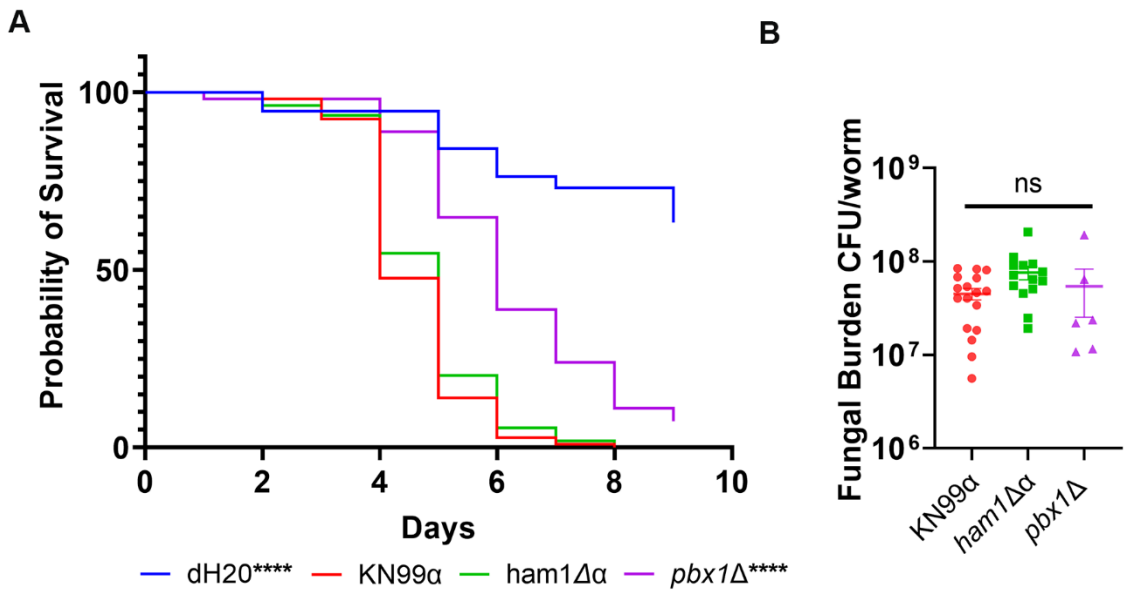

Figure 2.5 *ham1*Δα shows no difference capacity compared to wildtype in *G. mellonella* A) Kaplan-Meier survival curve of KN99α (n=107), *ham1*Δα (n=108), and *pbx1*Δ (n=54). One-way ANOVA with a Dunnet's multiple comparison test ****p<0.0001. B) Fungal burden assessment of infected worms. A One-way ANOVA was run with a Dunnet's multiple comparisons test of mutants to WT (KN99α n=17, *ham1*Δα n=15, *pbx1*Δ n=6).

3.3.6 Multiple deletions of *ham1*Δ, including a commercial strain (C07), behave similarly to *ham1*Δα in several virulence specific assays.

Because we were unable to obtain an in-locus complemented strain, to increase rigor, we assessed mating phenotypes of the commercial *ham1*Δ mutant C07 in addition to our own independent *ham1*Δ strains (see Chapter 2.3.6). Following the same logic, we wanted to use the C07 mutant to assess key virulence phenotypes that we have observed in our *ham1*Δ mutants. When assessing capsule integrity, C07 also showed a defect, retaining a similar amount of capsule post-sonication as our *ham1*Δα (Fig. 2.6 A).

When looking at biofilm production, we see a similar trend that more biofilm is produced relative to the WT strain (Fig. 2.6 B). When assessing exopolysaccharide release, we saw no significant differences from WT, like we did with our own *ham1*Δα mutant, although C07 trends towards more shedding across all conditions (Fig. 2.6 C-E).

When assessing capsular transfer, we see a similar phenotype to our *ham1*Δα where C07 had difficulty with capsule transfer at dilutions greater than 1:750. Finally, when looking at survival and fungal burden in *G. mellonella*, we observe no difference in median survival or CFU burden (Fig. 2.6 F, G). By using the independently generated C07 mutant, we are able to provide additional confidence to the phenotypes we have observed in our *ham1*Δ mutants.

Fig. 2.6 Assessment of virulence phenotypes using commercial deletion mutant C07. A) C07 has similar defects in capsule attachment to *ham1*Δ mutants' post-sonication. A One-way ANOVA was run using a Dunnett's multiple comparison test of all mutant crosses to the WT cross ** p=0.0062 (*ham1*Δα) **, p=0.0040 (C07), ***p=0.0004. n= 20 cells for all conditions. B) C07 sheds similar amounts of capsule to WT in non-capsule inducing media YPD. A One-way ANOVA was run with a Dunnett's multiple comparisons of mutants to WT *p=0.0254. C) C07 sheds similar amounts of capsule to WT in minimal media YNB. A One-way ANOVA was run with a Dunnett's multiple comparisons of mutants to WT. D) C07 trends towards shedding more capsule in capsule inducing media DMEM. A One-Way ANOVA with a Fisher's LSD test was run on all samples * p=0.0321. n=3 biological replicates for all ELISAs. E) C07 shows no difference in survival compared to WT. Kaplan-Meier survival curve of mq$H_2$0 (n=10), KN99α (n=30), *ham1*Δα (n=30), and C07 (n=30). A One-way ANOVA with a Dunnet's multiple comparison test of all conditions to WT. No differences were seen in the mutants but the mq$H_2$0 survived significantly longer ****p<0.0001. F) C07 (n=11) shows no difference in fungal burden compared to KN99α (n=7) or *ham1*Δα (n=7). A One-way ANOVA with a Dunnet's multiple comparison test of all conditions to WT was run and showed no significant difference between mutants and WT. G) C07 fails to fully transfer capsule at high dilutions greater than 1:750. Representative images of capsule transfer capsule visualized by conjugated 3C2 antibody with Alexa488 fluorescent probe and cell wall stained with Calcofluor white (CFW) scale bar is 10um.

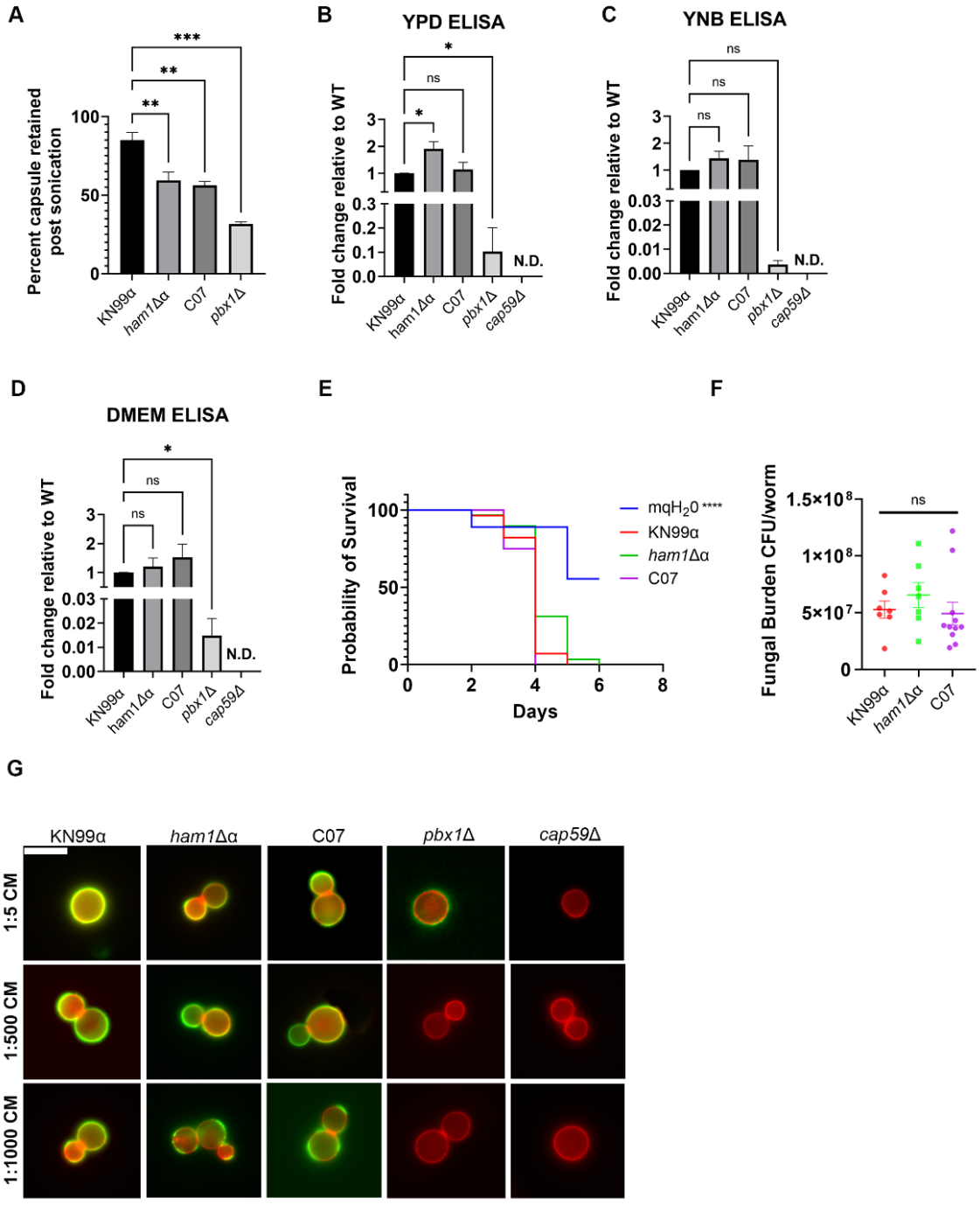
A
Percent capsule retained post sonication
100
50
0
***
**
**
KN99α
ham1Δα
C07
pbx1Δ
B
YPD ELISA
Fold change relative to WT
3
2
1
0.3
0.2
0.1
0.0
*
ns
*
N.D.
KN99α
ham1Δα
C07
pbx1Δ
cap59Δ
C
YNB ELISA
Fold change relative to WT
3
2
1
0.03
0.02
0.01
0.00
ns
ns
ns
N.D.
KN99α
ham1Δα
C07
pbx1Δ
cap59Δ
D
DMEM ELISA
Fold change relative to WT
3
2
1
0.03
0.02
0.01
0.00
*
ns
ns
N.D.
KN99α
ham1Δα
C07
pbx1Δ
cap59Δ
E
Probability of Survival
100
50
0
0
2
4
6
8
Days
mqH20 ****
KN99α
ham1Δα
C07
F
Fungal Burden CFU/worm
1.5×10^8
1×10^8
5×10^7
0
ns
KN99α
ham1Δα
C07
G
KN99α
ham1Δα
C07
pbx1Δ
cap59Δ
1:5 CM
1:500 CM
1:1000 CM

3.4 Discussion

Given that our results are consistent with *HAM1* having a role in fungal mating, and that others have shown a clear link between mating and virulence, we were interesting on testing if *HAM1* also had a connection to virulence, especially when we found that *HAM1* transcripts were some of the highest induced in the cerebral spinal fluid (CSF) of cryptococcosis patients (Yu et al., 2021, Chen et al., 2014). Our initial survey of the key virulence mechanisms did not show any obvious defects in *ham1*Δ mutants. Still, we decided to take a closer look at the capsule since, as a downstream target of Pfa4, it's possible that *ham1*Δ may share defects related to the cell wall or capsule as exhibited by the *pfa4*Δ. Additionally, since one of the major phenotypes in the *ham1*Δ relates to filamentation, we wanted to investigate if there was a possible cross over between the cellular circuits governing morphology and capsule production and maintenance.

The polysaccharide capsule is a vital virulence factor for survival inside the host. The capsule is composed of galactoxylomannan (GalXM), mannoproteins, and glucuronoxylomannan (GXM) (Crawford et al., 2020). GXM constitutes 90% of the capsule mass and has been implicated in interference of host immunity, prevention of phagocytosis, and inhibition of leukocyte migration and cytokine production (Crawford et al., 2020, Denham et al., 2017). Believed to be functioning as cell wall remodelers, parallel beta helix 1 and 2 deletion strains (*pbx1*Δ and *pbx2*Δ) exhibited reduced capsule attachment ability, reduced capsule synthesis, and reduced capsule transfer, all resulting from abnormal capsule structure (Liu et al., 2007, Kumar et al., 2014). These mutants are also attenuated in virulence, highlighting the importance of correct capsule function for pathogenesis.

With such well-defined capsule phenotypes, we used the *pbx1*Δ strain as a positive capsule mutant control to investigate the capsule integrity of *ham1*Δα. Although capsule induction was similar, *ham1*Δ mutants exhibited a defect in capsule attachment and shedding. This was similar to phenotypes exhibited by *pbx1*Δ and *pbx2*Δ strains, both mutants with abnormal capsule structure (Liu et al., 2007, Kumar et al., 2014). This suggested a level of involvement of *HAM1* in proper capsule formation. While defects were milder than *pbx1*Δ, capsule attachment and transfer were reduced in the *ham1*Δ.

Capsular shedding, however, was increased in our capsule non-inducing media YPD and trended towards higher shedding in capsule inducing medias. A previous study described the mutant *ima1*Δ as having increased capsular shedding ability in capsule inducing conditions while displaying normal capsule induction phenotypes (Denham et al., 2018). While the function of *ima1*Δ has yet to be fully elucidated, the similarities in capsular release to our *ham1*Δ could point to a similar function within virulence mechanisms. Capsule regulation and structure during mating conditions is a topic that has received little attention. Is reasonable to envision changes in capsule accompanying the morphological changes present during mating. In fact, a follow up study looking at the ZNF2^{OE} strain described in Chapter 1 found that the ZNF2^{OE} strain presents more antigens within the capsule than WT, and that if additional mutations are made to remove the capsule no protection is conferred when used as a vaccination (Lin et al., 2022). This discovery outlines a very clear difference in capsule produced by the hyphal form relative to the haploid yeast form. Since our *ham1*Δ mutants are prone to filamentation, these capsule defects seen in *ham1*Δ mutants might be a consequence of the abnormal mating signaling occurring in the absence of *HAM1*.

Biofilm production, while not seen as a virulence factor for *C. neoformans*, was likely developed as a survival tactic against environmental predation (Martinez et al., 2015). Altered biofilm production also points to defects in capsule release and/or altered capsule structure, which was apparent in our *pbx1*Δ and *ham1*Δα mutants as both produced larger biofilms. With all the similarities in capsule defects shared between *pbx1*Δ and *ham1*Δα, we next wanted to assess the virulence capabilities of *ham1*Δ.

Deletion of *pbx1*Δ results in attenuated virulence in a mouse model so we expected to see a similar defect in our *ham1*Δα (Liu et al., 2007). To our surprise, there were no significant defects in virulence potential using the *G. mellonella* infection model although we observed a delay in the median death rate for our *ham1*Δα relative to our WT (WT, 4 days; *ham1*Δα, 5 days; and *pbx1*Δ, 6 days). Still, there were no differences in fungal burden at time of death, even in the *pbx1*Δ-infected worms. This could be attributed to the fact that they lived longer, as the burden was assessed at time of death. More detailed virulence assays will be needed to confirm if there are defects in *ham1*Δ mutants affecting its pathogenesis, such as determination of fungal burden over time.

Our studies of *HAM1* in *C. neoformans* biology have shown another intersection point between virulence and mating. Both processes are vital to the propagation and survival of the species and the presence of regulators with roles in multiple pathways reflects just how important these are. Investigation of mating regulators not only improves our knowledge of how the system works but also opens new avenues of investigation to therapeutic interventions. Through a better understanding of fungal mating, we may be able to find more intersection points between virulence and mating pathways to fully understand

how these two processes are connected. We hope this serves to raise awareness about the importance of mating for virulence and stirs more investigations into this phenomenon.

3.5 Methods

3.5.1 Capsule induction and visualization with India ink

Cultures were grown overnight in 5 mL of YPD medium. Cultures were spun down at 3,000 x g for 5 minutes and resuspended in 1 mL of PBS. After cell count, $1x10^7$ cells/mL were transferred to a new microtube and pelleted. Pellet was resuspended in 1 mL of Dulbelcco's Modified Eagle's Medium (DMEM) (Corning; VWR 45000-304). This suspension was diluted 10-fold by adding 500 uL to 4.5 mL of DMEM to a final concentration of $1x10^6$ cells/mL. 1 mL aliquots of this cell suspension were added into a 24 well culture plate and incubated at 37°C with 5% CO_2 for 24 hours. After 24-hour incubation, samples were transferred to microtubes and spun down at 3,000 x g for 5 minutes. Samples were washed in PBS and resuspended in a final volume of 50 uL. In a separate tube, 10 uL of sample were mix with India Ink and a drop of the mixed sample and India ink was pipetted onto a Polylysine-coated slide and imaged on a Zeiss Axio Observer Microscope.

3.5.2 Capsule sonication

Capsule is induced as described above and cells were resuspended in 1 mL of 1x PBS. A portion of the cells was aliquoted (unsonicated controls) and the rest were subjected to sonication using a tip sonicator (Branson #SFX250) at 20% power with 0.5 pulse for 20s and kept on ice. Once all strains had been sonicated, all samples were mixed with India ink as described above and visualized on a Zeiss Axio Observer Microscope at 100x oil immersion magnification. The capsule radius was measured using FIJI (Abramhoff et al., 2004).

3.5.3 Capsule transfer

Capsule transfer assays were performed as previously described by Kumar et al., 2014. Capsule donor strains were grown in 5 mL of YPD liquid culture for 5 days prior to the experiment. On day 4 a *cap59Δ* acceptor culture was grown overnight. Donor cultures were spun down for 5 minutes at 3,000 x g and the top 1.5 mL was filtered through a 0.22μm filter (avantor #76479-024). 1 mL from this filtration step was heated at 70C to create conditioned media. Acceptor cells were washed twice with 1x PBS and counted on a Bio Rad TC20 automatic cell counter and diluted to final concentration of $5x10^6$ cells/mL in a volume of 400ul.

Conditioned media was added in the appropriate dilution to acceptor cells and incubated for 1hr with gentle rotation. Cells were pelleted at 3000 x g for 5 minutes and washed twice with 1x PBS. Resuspend cells in a volume of 100 uL and added Cy3 conjugated 3C2 anti GXM antibody to a final concentration of 8ug/ml. Incubated for 1 hour with gentle rotation. Cells were pelleted at 3000 x g for 5 minutes and washed twice with 1x PBS. Cells were resuspended in 100 uL and 100 ug/mL concentration of CFW was added and incubated for 20-30 mins with gentle rotation. Cells were pelleted at 3000 x g for 5 minutes and washed twice with 1x PBS. Cells were resuspended in a final volume of 50 uL of 1x PBS.

3.5.4 Capsule shedding and GXM immunoblotting:

GXM immunoblotting assays were performed as previously described (Yoneda and Doering 2008, Denham et al., 2018). Briefly, cells were inoculated into YPD and allowed to grow for 24 hours. Subsequently dilutions of 1:100 were performed and cells were

inoculated into the desired media of interest with the exception of DMEM where $1x10^6$ cells/mL were added to 5 mL of fresh DMEM. Cells were then incubated in their respective medias for 3 days at 30°C with shaking at 225 rpm. DMEM cultures were incubated at 37°C with 5% $C0_2$ to induce capsule formation and subsequent shedding. After 3 days, the cultures were quantified on a cell counter (Bio-Tad TC20), and the whole culture were spun down for 5 minutes at 3000 x g.

The top 1.5 mL was filtered through a 0.22μm filter. 1 mL from this filtration step was heated at 70°C for 10 minutes to create conditioned media. Subsequent conditioned media was loaded onto a 0.6% Megabase agarose gel (BioRad #1613108) and run for 8-10 hr at 40V. To normalize the amount of GXM loaded onto the gel, cell counts were taken for each strain in each media. The amount of GXM loaded was normalized to the lowest cell count in a total volume of 100 ul. When the dye front was at the bottom of the gel, the electrophoresis was stopped and the gel used to assemble the immunoblot sandwich. Using a Nylon membrane, the sandwich was assembled as follows, starting from the bottom: wick, 3 pieces of thick blotting paper, gel, membrane, 3 pieces of blotting paper, and paper towels (approx. 5 cm in height). The immunoblot sandwich was incubated with a 20x Sodium Citrate buffer for 10-12 hours or until all the paper towels were saturated. The membrane was blocked for 48 hours in 1× TBS-5% milk and incubated for 1 h in 1×TBST-1% milk with 1 μg/mL of anti-GXM monoclonal antibodies F12D2 and 1255. The membrane was rinsed three times in 1× TBST and incubated for 1 h in 1× TBST-1% milk with Odyssey antibody at 1:10,000. The membrane was rinsed again three times in 1× TBST and imaged on the Odyssey Imaging System (LI-COR).

3.5.5 Capsule shedding via ELISA

ELISA protocol was followed using the kit insert provided by IMMY-Labs (#CRY101). Conditioned media from cells was obtained as previously described for GXM immunoblots. Conditioned media was diluted by a factor of $1x10^{-4}$ and $1x10^{-6}$ using serial dilutions due to the sensitivity of the assay. Lyophilized GXM was provided by the Brown Lab at the University of Utah and diluted to a concentration of 2mg/mL and working stocks were generated. The highest standard used in the ELISA was 78 ng/mL.

3.5.6 XTT Biofilm Assay

Assay was performed as previously described (Pierce et al., 2008). Strains were grown overnight in YPD, cells were then counted (Bio-Rad TC20 automatic cell counter) and diluted to $1x10^{7}$ cells/mL in DMEM, and 100ul of all of cell suspension was seeded into wells of a microtiter plate. Plates were incubated at 37ºC + 5% CO_2 for 48 hr, washed with 1x PBS using a microtiter plate washer (405LS, Agilent), and 100 µl of XTT/menadione solution (Sigma) was added to each well. The plates were incubated for 3 hr and 75 µl of the supernatant was removed and transferred to a new microtiter plate. Plates were read in a microtiter plate reader at 490 nm.

3.5.7 Uptake Assay

Uptake assays were performed as previously described (Santiago-Tirado et al., 2015). PMA-differentiated THP-1 cells were incubated with Lucifer Yellow-stained fungal cells that had been opsonized with 40% Human serum collected from healthy donors

(approved by the Notre Dame Institutional Review Board (IRB) as a non-human subject research procedure). After incubation for 1 hour at 37°C with 5% $C0_2$, plates were washed with 1x PBS using a microplate washer (405LS, Agilent). Cells were then fixed with 4% Formaldehyde and stained with DAPI (Sigma) and Cell Mask (Invitrogen). NaN_3 in PBS was added to the plates and imaged on a Zeiss Axio Observer Microscope with an automatic stage. Each well was imaged using a 3x3 grid set up and resulting images were analyzed using a Cell Profiler pipeline to determine the Phagocytic Index (PI) values.

3.5.8 Infections with *G. mellonella*

G. mellonella third instar larvae were sorted and weighed as described by Stempinksi et al., 2022. Larvae weighing 200 mg and above were used in the following infection assay. Overnight cultures were grown and measured for an OD of 0.5-1. Cells were then washed 2x in 1x PBS and counted using a cell counter. A total inoculum of $1x10^5$ cells/larvae was used in a total of 5ul. The back larval prolegs were swabbed with 70% Ethanol and 5ul of culture was injected into the back right proleg using a Hamilton Syringe (Hamilton, #80300). Syringes were sanitized and cleaned before and after each strain with both 70% Ethanol and dH_2O.

3.5.9 Assessment of Fungal burden with *G. mellonella*

At time of death, infected *G. mellonella* larvae were placed in 3 mL of dH_2O in a 15 mL falcon tube. Larvae were then homogenized using a tissue homogenizer (VWR #10032-336) to break down tissue. Once sufficiently homogenized, worm slurry was then diluted 10,000 or 20,000x times and plated on YPD plates supplemented with either Nourseothricin (NAT) and Ampicillin (AMP) or Gentecin (G418) and Ampicillin (AMP).

Plates were left to incubate for 2-3 days and then imaged on the Biorad EZ Gel Doc imager for CFU quantification.

CHAPTER 4:

MAJOR CONCLUSIONS AND FUTURE DIRECTIONS

4.1 Major Conclusions of *HAM1* involvement in *C. neoformans* biology

Our investigation of *HAM1* involvement in *C. neoformans* biology has revealed a dual role in both mating and virulence. When looking at fungal mating, our studies suggest that *HAM1* acts as a negative regulator of mating due to the hyper progeny generation and hyphal production of *ham1*Δ mutants (Fig. 1.1 A, 1.2 A). While we were unable to uncover the specific location of *HAM1* within the mating cycle, we propose that it could be acting in three possible locations (Fig. 3.1). First, it could be somewhere within the pheromone response pathway as this comprises the initial processing of the pheromone signal which allows for the mating process to start. Second, directly after pheromone-dependent transcription as this is a crucial step in which other downstream targets are activated to start the morphological transitions. Or third, the direct yeast to hyphal transition, given the phenotype of the *ham1*Δ mutants to form hyphae it's possible that *HAM1* could be an additional check point at this stage (Fig 3.1).

Our rationale for investigating potential virulence connections started with our hyper filamentation phenotype and capsule defects shown by our mutant. We wanted to test if there was a possible cross over between the cellular circuits governing morphology and capsule production and maintenance. Our findings have concluded that there is some connection between these two pathways due to the defects we observed in capsule attachment and transfer as well as increased exopolysaccharide release and biofilm

production (Fig. 2.3 A and C, Fig. 2.4). These capsular abnormalities suggest that *HAM1* may be important for proper cell wall to capsule interactions (Fig. 3.1).

When we think about these roles in the context of pathogenesis, we believe that *HAM1* prevents mating from happening in the low nutrient environment of the host and reinforces capsule integrity by preventing mating morphological transitions from occurring (Fig. 3.1). This could be a potential reason for why *HAM1* is so highly expressed in the CSF of patients. CSF is a very nutrient limited environment which may provide the right pressures for cells to undergo a mating interaction, which would be detrimental for pathogenesis.

Our data regarding the role of *HAM1* in *C. neoformans* biology is consistent with the idea that mating and virulence are connected. One of the fundamental issues with creating targeted therapies for fungal infections is the fact that they possess many similarities to mammalian cells and as such can have very harsh side effects. The fungal mating pathway is one avenue that can be explored more deeply for unique targets and with a clear connection to virulence could serve as a way to treat these devastating infections.

While we were able to uncover what pathways *HAM1* may be involved in, more work is needed to define its exact location within mating and virulence pathways. In the remainder of this chapter, we have described some future directions for how to proceed with defining the role of *HAM1* in mating and virulence.

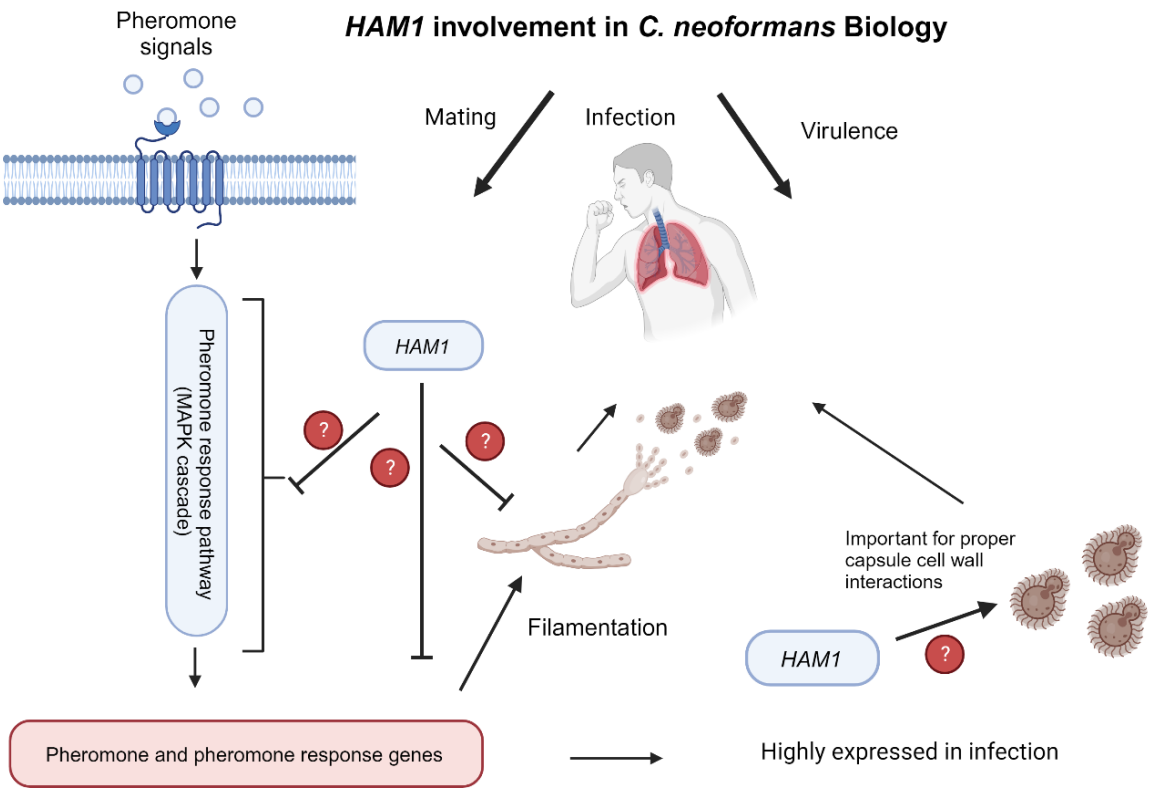

Figure 3.1 Proposed model of *HAM1* involvement in C. neoformans Biology**.** Based on what we have learned we believe that *HAM1* acts as a negative regulator in the mating cycle of C. neoformans. It may be acting on the pheromone response pathway, on the pheromone and pheromone response genes directly, or somehow inhibiting hyphal formation directly. When looking at virulence we found defects in capsule attachment and release suggesting that *HAM1* may be important for capsule cell wall attachment. In pathogenic conditions, we believe that *HAM1* may be highly expressed to prevent the morphological transition to a hyphal from occurring due to the low nutrient environment of a mammalian host. This figure was created with BioRender.com.

4.2 Future Directions for characterization of *HAM1*

4.2.1 Generation of additional *HAM1* strains for future studies.

When considering future directions for this project, a few additional strains are needed to provide rigor to support our findings thus far, and to support follow-up studies. One of the first strains that would be important to construct is a complement to our *ham1*Δ. A complement provides confidence that the phenotypes that we are seeing from our deletion strains are in fact as a result of deleting *HAM1* itself rather than off-target effects. Our efforts to construct an in-locus complement by biolistic techniques were unsuccessful. However, recently the Madhani group published a CRISPR-cas9 technique that could be used to replace the resistance marker cassette in our *ham1*Δ mutants at the endogenous location of *HAM1* with a functional copy of *HAM1* containing a resistance marker cassette downstream of the terminator sequence (Huang et al., 2022). If we are unable to successfully complement endogenously using this technique, we could still use our *ham1*Δ mutants and send the constructed *HAM1* and resistance marker cassette to an intergenic safe haven region which has been previously shown to be an effective strategy for complementation (Arras et al., 2015).

One of the biggest questions we have at the end of this study is where is *HAM1* during mating and virulence conditions? One way we can start to get answers to this question is by looking at where a fluorescently tagged Ham1 localizes in the cell. We can use the same CRISPR-cas9 system as described above to add a fluorescent tag to the endogenous location of *HAM1* (Huang et al., 2022). After generating this strain, we can visualize where Ham1 is localizing under different conditions.

When discerning the function of *HAM1* we took the approach of looking at phenotypes that occur when it is absent. However, a direction we could also consider in follow-up assays is overexpression. Characterization of morphological regulator *ZNF2* are a perfect example of how deletion and overexpression can result in very different phenotypic outcomes (Section 1.4.1) (Lin et al., 2010). Additionally, we know that *HAM1* is highly expressed in patient CSF, its possible that overexpression of *HAM1* may shed some light on why this might be the case (Yu et al., 2021, Chen et al., 2014). We can generate an overexpression mutant in a few ways, first we could use the CRISPR-cas9 system to target the promoter region of endogenous *HAM1* and replace it with the Actin promoter for constant expression. Alternatively, we could send a second copy of the *HAM1* sequence to the intergenic safe haven as described above (Arras et al., 2015). However, if *HAM1* overexpression results in lethality, we can also use an inducible promoter system. In this case, we can replace the *HAM1* endogenous promoter with an inducible promoter such as the Galactose or Copper promoter (Baker et al., 2014, Ory et al., 2004). In this case, the absence of galactose or presence of copper, respectively, will repress the gene, while addition of galactose or copper chelation, will overexpress the gene. Generation of these three strains, the complement, the fluorescent tagged, and the overexpression strain of *HAM1*, will allow us to gain a more comprehensive knowledge and add additional scientific rigor to our findings of what and where *HAM1* is acting in mating and non-mating conditions.

4.2.2 Visualization of Ham1 in mating and non-mating conditions

By generating a fluorescently tagged *HAM1* strain, we will be able to determine where Ham1 is localizing in mating and non-mating conditions. This can inform other analyses such as determining binding partners and pinpointing specific pathways where *HAM1* is involved.

4.2.2.1 Mating conditions

The best way to test localization in a mating specific manner would be to set up a bisexual cross with our new tagged strain. V8 media is only used in a solid agar plate form, so a bisexual mating assay with KN99a x *HAM1*:mNeon-MATα would be set up, scraped and visualized at various time points. Since a small amount of sample would be needed for visualization solid agar plating should be sufficient and allow for ease of testing different stages of the mating cycle.

4.2.2.2 Non-mating conditions

To assess where Ham1 may be localizing in non-mating conditions several different medias should be tested to take a look at a full range of *in vitro* conditions. To look at "normal" growth conditions YPD would be best to look at robust growth due to the nature of this rich media. For host like conditions DMEM+ 5% CO_2 and artificial CSF (aCSF) should be tested. DMEM + 5% CO_2 is standard practice in the field for *in vitro* approximation of host like conditions and aCSF would be useful based on the fact that *HAM1* is one of the most highly expressed transcripts in patient CSF.

4.2.3 RNA-seq profiling of *HAM1* in mating and non-mating conditions

RNA-seq allows us to understand what is happening transcriptionally in a cell in "real time". This could tell us what other genes are affected in the absence of *HAM1* under different media conditions. For these assays, however, we would need a complemented strain to ensure rigor during the analysis.

4.2.3.1 Mating conditions

To assess what is happening during mating conditions there are two different media approaches that could be used. Bisexual mating assays would be set up between KN99α x KN99a (WT), *ham1*Δα:*HAM1* x KN99a (complement) and *ham1*Δα x *ham1*Δa (mutant) on solid V8 agar plates and then scraped at the appropriate time-point and RNA extracted. By testing the complement, we ensure that any differences in transcriptional profiling are solely due to the deletion of *ham1*Δ and provide an additional layer of scientific rigor to this assay. It would be best to do these analyses in a time course to take a look at how the mating cycle progresses over time and where *HAM1* exerts the greatest effects. Solid media has the caveat of having limitations on how much volume of culture can be plated. MS media has been used in both liquid and solid form in other applications but is mostly in *C. deneoformans* and would require optimization for our strains (Ramage et al., 2008, Adelberg et al., 2010). A series of liquid MS cultures could be set up and pulled at appropriate time points and RNA extracted.

As we saw with our qPCR analysis, not all cells in *C. neoformans* strains will enter into a mating interaction. As a result, our RNA-seq analysis is likely to be noisy. However, we can also test the sister species to *C. neoformans*, *C. deneoformans*, which is

very prone to mating, and investigate if *HAM1* is also involved in the mating cycle. We did not find any discernable phenotypes in mutants generated in *C. deneoformans* strains JEC21 and JEC20 but there may be differences transcriptionally that were not accounted for phenotypically.

4.2.3.2 Non-mating conditions

Using RNA-seq to assess *HAM1* transcriptional activity in non-mating conditions, could be useful in identifying other genes that are differentially expressed in the absence of *HAM1* during normal and host-like condition growth parameters. This would allow us to target our search to potential binding partners under these different conditions. For all experiments KN99α, *ham1*Δα and our *ham1*Δα:*HAM1* complemented strain would be grown in liquid culture under defined time parameters and RNA extracted. Consistent with parameters used for visualization, YPD would be best for robust growth and non-stress conditions, for host like conditions DMEM+ 5% CO_2 and aCSF should be tested which will provide a comprehensive look at what might be happening in a mammalian host setting.

4.2.4 Binding partner analysis using Ham1-FLAG tagged strain

Using our previously generated Ham1-FLAG tag strain we can do an immunoprecipitation paired with Mass Spectrometry (Co-IP/MS) to identify proteins that interact with our Ham1-FLAG. While running our IP paired with a click chemistry reaction, one issue we ran into was the low percentage of the protein that was able to be pulled down (Section 2.3.1). With the workflow we had we were able to obtain the information we needed with a low percent pull down, however this may not produce

enough product to get useful information out of a traditional LC/MS workflow. One possibility for this low pull-down efficiency could be that the FLAG-tag is being cleaved in the pull-down process and as such is binding to the beads with no useable protein products attached. A possible solution to removing these FLAG peptides is to add a Field Asymmetric Ion Mobility Spectrometry (FAIMS) step prior to downstream Mass Spectrometry analysis. FAIMS allows for greater depth in protein coverage which could assist in getting better results from our LC/MS workflow (Ang et al., 2022). Briefly, FAIMS works by having 2 electrodes with alternating high and low electric fields between them. This allows for gas phase separation of ions by differences in mobility in both high and low electric fields (Ang et al., 2022, Kolakowski and Mester, 2007). This method of separation results in a filtering out of undesirable singly charged and contaminating ions i.e., FLAG tag peptides, allowing for greater coverage of less abundant proteins that would be harder if not impossible to detect without removal of the FLAG peptides (Ang et al., 2022).

If the resources are available, a previous study looking at a yeast proteome devised a strategy using FAIMS coupled with nano-LC/MS (Swearingen et al., 2012). The advantage of using nano-LC/MS over traditional LC/MS is that it allows for high resolution of sample products in either limited sample or complex sample conditions (Gaspari and Cuda, 2011). Due to the complexity of subjecting Ham1-FLAG cells to a mixed culture environment, if nano-LC/MS is available this might be the best downstream Mass Spec strategy to ensure good results.

4.2.4.1 Mating conditions

In order to induce mating conditions in our *C. neoformans* strains, we would have to use a bisexual mating scenario. Our previously generated Ham1-FLAG strain is in the MATa background. Attempts were made to also generate a strain in the MATα background but these were unsuccessful when tested using a western blot. By using the previously described CRISPR-cas9 system for visualization of Ham1, it's possible that there might be greater success in generating a Ham1-FLAG strain in the MATα background (Huang et al., 2022). It would be important to test both MATα and MATa backgrounds due to the differences we found in specific mating assays. By assessing binding partners in both MAT strains we could find out if *HAM1* acts depending on the background.

These crosses could be set up on solid V8 agar plates or possibly with liquid MS media as described in section 2.3.1 depending on efficacy of the mating interactions with liquid MS. With the knowledge that not all cells will enter into a mating interaction, it would be best to use a longer time point scheme initially to ensure that the majority of the Ham1-FLAG cells will enter into mating interactions. Alternatively, if this did not interfere with downstream processing dosing crosses with 7.5μM of exogenous MATα pheromone used for our cellular fusion experiments could assist in enhancing mating efficiency.

4.2.4.2 Non-mating conditions

Using the same experimental design as our mating conditions, it would be interesting to see what binding partners are present in normal growth (YPD) and host like conditions

(DMEM+ 5% $C0_2$ and aCSF). By looking at who Ham1 is interacting with we may be able to pinpoint which cellular circuits it has additional roles in beyond mating. This may also help shed light on why we see capsular phenotypes in our *ham1*Δ mutants.

4.2.5 Yeast-2-Hybrid analysis of binding partners

Once we have defined a list of possible binding partners from our LC/MS workflow we can use a Yeast-2-Hybrid assay to confirm if these are true binding partners. Briefly, two plasmids are constructed called bait and prey (Fields and Song 1989, Bruckner et al., 2009). These two plasmids are then co-transfected into yeast and if there is a positive interaction, reporter genes are transcribed that enable growth on a specific media or a colorimetric change is observed (Fields and Song 1989, Bruckner et al., 2009).

One of the pieces of information that initially caught our attention about the Ham1 protein was one of the protein domains. As noted in the initial discovery in connection with Pfa4, Ham1 contains a domain of unknown function, DUF4449, a domain that is unique to fungi (Santiago-Tirado et al., 2015). This is intriguing from a potential therapeutic standpoint and as such should be investigated further when looking at binding partner interactions.

A recent search for updates on annotated protein features revealed that an additional DUF domain has been assigned to Ham1, DUF5923 which is also a domain that is unique to fungi (Fig. 3.2). We can test if either of these DUF domains are important for binding partner interactions by constructing plasmids that have these DUF domains alone and assess binding partner interactions.

4.2.5.1 Mating conditions

Taking our list of previously identified binding partners from our LC/MS workflow, two separate Y2H workflows should be set up to look at MATα vs MATa binding partner interactions. Several bait plasmids should be constructed for all assays, first a full length *HAM1* sequence followed by independent plasmids looking at the two DUF domains of interest. This will not only help us to identify which one is important for partner binding but will also provide one function that these domains serve in fungal biology. Prey plasmids should be constructed based on available knowledge of predicted binding domains to start this assessment.

4.2.5.2 Non-mating conditions

Similar to the approach for mating conditions, it's possible that there a different binding partners for Ham1 depending on the media condition. If this is the case several workflows should be set up to test these various interactions starting with the two bait plasmids described above. If the resources are available, an interaction mating Y2H could be useful to screen a large amount of different bait and prey plasmids to maximize efficiency (Roberts et al., 2011).

Vectors for expressing bait and prey protein encoding sequences are put into different haploid yeast strains of opposite mating type (Roberts et al., 2011). To test for an interaction these two strains are mated together to produce diploids that can then be screened for reporter genes (Roberts et al., 2011). Once these haploid strains are generated, they can be stored as libraries in 96 well plates and manipulated in a plate setting for initial mating and subsequent reporter screening (Roberts et al., 2011).

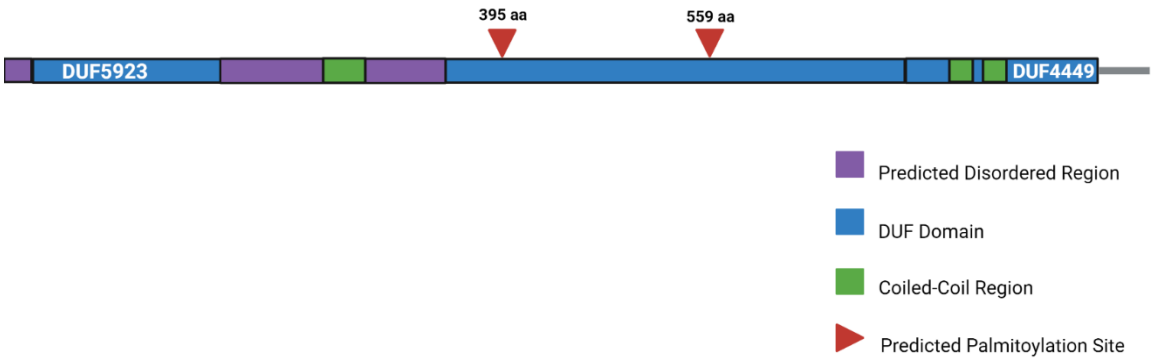

Figure 3.2 Annotated protein features of Ham1. Illustration set to scale of DUF domains and other predicted protein features of the Ham1 sequence. All protein features were obtained from Interpro (https://www.ebi.ac.uk/interpro/) database under the FungiDB entry for Ham1 (CNAG_02129). Predicted palmitoylation sites were also added from the GPSPalm prediction software (https://gpspalm.biocuckoo.cn/). This illustration was created using Biorender.

4.2.6 Phenotypic assessment of double knockout mutants to pinpoint exact location of *HAM1* in specific pathways

After confirming binding partners for Ham1 from our Y2H assay, we will prioritize a list of genes to follow up by using database resources such as FungiDB to find more information on these binding partners, especially expression profiles. With these data we will be able to generate a list of higher confidence hits to explore. From this shortened list of binding partners we can generate a series of double knockout mutants to pinpoint the exact location of *HAM1* in cellular pathways for both mating and non-mating conditions. Phenotyping of these double mutants will help to define the dual role that *HAM1* plays in *C. neoformans* biology. We expect that, due to the mounting success we have had in our lab using the CRISPR-cas9 system from the Madhani lab for generating knockouts, creating new double knockout strains using our existing *ham1*Δα and *ham1*Δa as a backbone should be successful (Huang et al., 2022).

4.2.6.1 Mating conditions

After generating double knockout mutants in both MATα and MATa backgrounds, cellular fusion and hyphal formation should be tested to see what affects the additional mutation have on these assays. These two mating assays generated the largest differences as compared to WT during our initial investigations. Any variation from what we have seen previously in our *ham1*Δ strains would provide valuable insight in pinpointing where *HAM1* may be acting in the mating pathway.

4.2.6.2 Non-mating conditions

A similar approach should be taken for our non-mating conditions, with the exception that only the MATα background needs to be assessed due to the clinical relevance of MATα vs MATa. In terms of initial assays to use, capsule attachment and biofilm are both excellent options due to their low cost, speed of completion, and clear phenotypic difference in the *ham1*Δ.

4.2.7 Site directed mutagenesis of predicted palmitoylation sites and functional impacts

We were able to confirm that Ham1 is a palmitoylated protein but we have not determined what impact palmitoylation has on the function of Ham1. One way that we can test this is by performing site directed mutagenesis on the predicted palmitoylation sites. Using our previously constructed plasmids for our *HAM1*:mNeon strain for visualization, the Agilent (formerly Stratagene) QuickChange Site Directed Mutagenesis kit can be used to alter the palmitoylation sites in a 1, 2, and 1+2 format to generate 3 independent strains (Klutts et al., 2007). These mutant strains can be confirmed by our previously described IP coupled to a click chemistry workflow to confirm partial and complete loss of palmitoylation as well as through visualization (Section 2.3.1, Fig. 1.1).

4.2.7.1 Mating conditions

To assess if palmitoylation is necessary for Ham1's role in mating, cellular fusion and bisexual mating assays can be used to assess if the protein is still functioning properly. Since these are the key assays for our *ham1*Δ mutants, any phenotypic similarity between our mutant palmitoylation strains and the deletion mutants would confirm that palmitoylation is necessary for complete function of Ham1. Additionally,

since these strains will have a fluorescent marker, localization at different time points in the mating cycle can be assessed using culturing methods previously described.

4.2.7.2 Non-mating conditions

Along the same lines as mating conditions, palmitoylation may be important for the capsular phenotypes we found in our *ham1*Δ mutants. Therefore, capsule attachment and biofilm production should be assessed in comparison to our *ham1*Δ mutants. As was stated previously for our mating conditions, localization can also be assessed under different culturing conditions i.e. YPD, DMEM + 5% $C0_2$ and aCSF. It may also be beneficial to look at some cell membrane stressors such as SDS to see if our palmitoylation mutants develop any new sensitivities.

4.2.8 Virulence testing in a mouse model

While we found no differences in virulence capacity in the *G. mellonella* wax worm model, it would be beneficial to move into a mouse model to confirm that there are no differences in virulence potential. The waxworm model is an excellent tool for screening different mutants, however, conditions used to rear larvae are not standardized among suppliers and as such variation in these factors can impact the immune system and decrease reproducibility of virulence experiments (Firacative et al., 2020). Running a mouse experiment eliminates some of these rearing standards and will allow us to assess dissemination and immune cell recruitment in response to different *HAM1* strains giving us a better picture of its involvement in mammalian infection. Additionally, since *HAM1* is one of the most highly expressed transcripts in patient CSF it's hard to believe that there is no impact on virulence.

Depending on what strains have been constructed prior to looking at virulence potential in mice, several experiments could be conducted. First, testing the *ham1*Δα mutant would be beneficial to see what impact *HAM1* has on virulence when absent. Second, depending on the phenotypic data from the palmitoylation mutants the single and the double mutants could have an effect on virulence potential. Third, it's possible that the virulence phenotypes we have observed *in vitro* and in our initial *in vivo* experiments did not capture why *HAM1* is so highly expressed in patient CSF, because it is the presence rather than the absence of *HAM1* that changes what occurs during infection. Therefore, it would be beneficial to construct an overexpression strain of *HAM1* and do an additional cohort of mice to test survival. For all mouse experiments it would be beneficial to do survival and CFU count of brain, lungs and spleen. If differences are seen in survival or CFU a follow up experiment focusing on histology could be useful to look at immune cell recruitment.

REFERENCES

1. Adelberg, J. W., Delgado, M. P., & Tomkins, J. T. (2010). Spent medium analysis for liquid culture micropropagation of Hemerocallis on Murashige and Skoog medium. *In Vitro Cellular & Developmental Biology-Plant*, *46*, 95-107.

2. Alanio, A., Desnos-Ollivier, M., & Dromer, F. (2011). Dynamics of Cryptococcus neoformans-macrophage interactions reveal that fungal background influences outcome during cryptococcal meningoencephalitis in humans. *mBio*, *2*(4). https://doi.org/10.1128/mBio.00158-11

3. Alvarez, M., & Casadevall, A. (2006). Phagosome extrusion and host-cell survival after Cryptococcus neoformans phagocytosis by macrophages. *Curr Biol*, *16*(21), 2161-2165. https://doi.org/10.1016/j.cub.2006.09.061

4. Ang, C. S., Sacharz, J., Leeming, M. G., Nie, S., Varshney, S., Scott, N. E., & Williamson, N. A. (2022). Getting more out of FLAG-Tag co-immunoprecipitation mass spectrometry experiments using FAIMS. *J Proteomics*, *254*, 104473. https://doi.org/10.1016/j.jprot.2021.104473

5. Arras, S. D. M., Chitty, J. L., Blake, K. L., Schulz, B. L., & Fraser, J. A. (2015). A Genomic Safe Haven for Mutant Complementation in Cryptococcus neoformans. *PLOS ONE*, *10*(4), e0122916. https://doi.org/10.1371/journal.pone.0122916

6. Baker, L. G., & Lodge, J. K. (2012). Galactose-Inducible promoters in Cryptococcus neoformans var. grubii. *Methods Mol Biol*, *845*, 211-226. https://doi.org/10.1007/978-1-61779-539-8_14

7. Barchiesi, F., Cogliati, M., Esposto, M. C., Spreghini, E., Schimizzi, A. M., Wickes, B. L., Scalise, G., & Viviani, M. A. (2005). Comparative analysis of pathogenicity of Cryptococcus neoformans serotypes A, D and AD in murine cryptococcosis. *J Infect*, *51*(1), 10-16. https://doi.org/10.1016/j.jinf.2004.07.013

8. Berger, A. (2000). Th1 and Th2 responses: what are they? *Bmj*, *321*(7258), 424. https://doi.org/10.1136/bmj.321.7258.424

9. Bicanic, T., Brouwer, A. E., Meintjes, G., Rebe, K., Limmathurotsakul, D., Chierakul, W., Teparrakkul, P., Loyse, A., White, N. J., & Wood, R. (2009). Relationship of cerebrospinal fluid pressure, fungal burden and outcome in patients with cryptococcal meningitis undergoing serial lumbar punctures. *Aids*, *23*(6), 701-706.

10. Botts, M. R., & Hull, C. M. (2010). Dueling in the lung: how Cryptococcus spores race the host for survival. *Curr Opin Microbiol*, *13*(4), 437-442. https://doi.org/10.1016/j.mib.2010.05.003

11. Botts, M. R., Giles, S. S., Gates, M. A., Kozel, T. R., & Hull, C. M. (2009). Isolation and characterization of Cryptococcus neoformans spores reveal a critical role for capsule biosynthesis genes in spore biogenesis. *Eukaryot Cell*, *8*(4), 595-605. https://doi.org/10.1128/ec.00352-08

12. Brückner, A., Polge, C., Lentze, N., Auerbach, D., & Schlattner, U. (2009). Yeast two-hybrid, a powerful tool for systems biology. *Int J Mol Sci*, *10*(6), 2763-2788. https://doi.org/10.3390/ijms10062763

13. Busse, O. (1894). Uber parasitare zelleinschlusse und ihre zuchtung. *Zentralbl Bakteriol*, *16*, 175-180. https://cir.nii.ac.jp/crid/1570291225300545280

14. Chen, Y., Toffaletti, D. L., Tenor, J. L., Litvintseva, A. P., Fang, C., Mitchell, T. G., McDonald, T. R., Nielsen, K., Boulware, D. R., Bicanic, T., & Perfect, J. R. (2014). The Cryptococcus neoformans transcriptome at the site of human meningitis. *mBio*, *5*(1), e01087-01013. https://doi.org/10.1128/mBio.01087-13

15. Chun, C. D., & Madhani, H. D. (2010). Applying genetics and molecular biology to the study of the human pathogen Cryptococcus neoformans. *Methods Enzymol*, *470*, 797-831. https://doi.org/10.1016/S0076-6879(10)70033-1

16. Crawford, C. J., Cordero, R. J. B., Guazzelli, L., Wear, M. P., Bowen, A., Oscarson, S., & Casadevall, A. (2020). Exploring Cryptococcus neoformans capsule structure and assembly with a hydroxylamine-armed fluorescent probe. *J Biol Chem*, *295*(13), 4327-4340. https://doi.org/10.1074/jbc.RA119.012251

17. Denham, S. T., Verma, S., Reynolds, R. C., Worne, C. L., Daugherty, J. M., Lane, T. E., & Brown, J. C. S. (2018). Regulated Release of Cryptococcal Polysaccharide Drives Virulence and Suppresses Immune Cell Infiltration into the Central Nervous System. *Infection and Immunity*, *86*(3), 10.1128/iai.00662-00617. https://doi.org/doi:10.1128/iai.00662-17

18. Dettmann, A., Heilig, Y., Valerius, O., Ludwig, S., & Seiler, S. (2014). Fungal communication requires the MAK-2 pathway elements STE-20 and RAS-2, the NRC-1 adapter STE-50 and the MAP kinase scaffold HAM-5. *PLoS Genet*, *10*(11), e1004762. https://doi.org/10.1371/journal.pgen.1004762

19. Fields, S., & Song, O.-k. (1989). A novel genetic system to detect protein–protein interactions. *Nature*, *340*(6230), 245-246.

20. Firacative, C., Khan, A., Duan, S., Ferreira-Paim, K., Leemon, D., & Meyer, W. (2020). Rearing and Maintenance of Galleria mellonella and Its Application to Study Fungal Virulence. *J Fungi (Basel)*, *6*(3). https://doi.org/10.3390/jof6030130

21. Fischer, M. S., & Glass, N. L. (2019). Communicate and Fuse: How Filamentous Fungi Establish and Maintain an Interconnected Mycelial Network [Review]. *Frontiers in Microbiology*, *10*. https://doi.org/10.3389/fmicb.2019.00619

22. Fu, C., Sun, S., Billmyre, R. B., Roach, K. C., & Heitman, J. (2015). Unisexual versus bisexual mating in Cryptococcus neoformans: Consequences and biological impacts. *Fungal Genet Biol*, *78*, 65-75. https://doi.org/10.1016/j.fgb.2014.08.008

23. Fu, C., Thielhelm, T. P., & Heitman, J. (2019). Unisexual reproduction promotes competition for mating partners in the global human fungal pathogen Cryptococcus deneoformans. *PLoS Genet*, *15*(9), e1008394. https://doi.org/10.1371/journal.pgen.1008394

24. Gaspari, M., & Cuda, G. (2011). Nano LC-MS/MS: a robust setup for proteomic analysis. *Methods Mol Biol*, *790*, 115-126. https://doi.org/10.1007/978-1-61779-319-6_9

25. Gyawali, R., & Lin, X. (2011). Mechanisms of uniparental mitochondrial DNA inheritance in Cryptococcus neoformans. *Mycobiology*, *39*(4), 235-242.

26. Hagen, F., Khayhan, K., Theelen, B., Kolecka, A., Polacheck, I., Sionov, E., Falk, R., Parnmen, S., Lumbsch, H. T., & Boekhout, T. (2015). Recognition of seven species in the Cryptococcus gattii/Cryptococcus neoformans species complex. *Fungal Genet Biol*, *78*, 16-48. https://doi.org/10.1016/j.fgb.2015.02.009

27. Heitman, J., Allen, B., Alspaugh, J. A., & Kwon-Chung, K. J. (1999). On the origins of congenic MATalpha and MATa strains of the pathogenic yeast Cryptococcus neoformans. *Fungal Genet Biol*, *28*(1), 1-5. https://doi.org/10.1006/fgbi.1999.1155

28. Herskowitz, I. (1989). A regulatory hierarchy for cell specialization in yeast. *Nature*, *342*(6251), 749-757. https://doi.org/10.1038/342749a0

29. Hsueh, Y. P., & Heitman, J. (2008). Orchestration of sexual reproduction and virulence by the fungal mating-type locus. *Curr Opin Microbiol*, *11*(6), 517-524. https://doi.org/10.1016/j.mib.2008.09.014

30. Huang, M. Y., Joshi, M. B., Boucher, M. J., Lee, S., Loza, L. C., Gaylord, E. A., Doering, T. L., & Madhani, H. D. (2022). Short homology-directed repair using optimized Cas9 in the pathogen Cryptococcus neoformans enables rapid gene deletion and tagging. *Genetics*, *220*(1). https://doi.org/10.1093/genetics/iyab180

31. Jung, K.-W., Lee, K.-T., So, Y.-S., & Bahn, Y.-S. (2018). Genetic Manipulation of Cryptococcus neoformans. *Current Protocols in Microbiology*, *50*(1), e59. https://doi.org/https://doi.org/10.1002/cpmc.59

32. Klutts, J. S., Levery, S. B., & Doering, T. L. (2007). A beta-1,2-xylosyltransferase from Cryptococcus neoformans defines a new family of glycosyltransferases. *J Biol Chem*, *282*(24), 17890-17899. https://doi.org/10.1074/jbc.M701941200

33. Kolakowski, B. M., & Mester, Z. (2007). Review of applications of high-field asymmetric waveform ion mobility spectrometry (FAIMS) and differential mobility spectrometry (DMS) [10.1039/B706039D]. *Analyst*, *132*(9), 842-864. https://doi.org/10.1039/B706039D

34. Kumar, P., Heiss, C., Santiago-Tirado, F. H., Black, I., Azadi, P., & Doering, T. L. (2014). Pbx proteins in Cryptococcus neoformans cell wall remodeling and capsule assembly. *Eukaryot Cell*, *13*(5), 560-571. https://doi.org/10.1128/ec.00290-13

35. Kwon-Chung, K. J., Bennett, J. E., Wickes, B. L., Meyer, W., Cuomo, C. A., Wollenburg, K. R., Bicanic, T. A., Castañeda, E., Chang, Y. C., Chen, J., Cogliati, M., Dromer, F., Ellis, D., Filler, S. G., Fisher, M. C., Harrison, T. S., Holland, S. M., Kohno, S., Kronstad, J. W., . . . Casadevall, A. (2017). The Case for Adopting the "Species Complex" Nomenclature for the Etiologic Agents of Cryptococcosis. *mSphere*, *2*(1), 10.1128/msphere.00357-00316. https://doi.org/doi:10.1128/msphere.00357-16

36. Kwon-Chung, K. J., Fraser, J. A., Doering, T. L., Wang, Z., Janbon, G., Idnurm, A., & Bahn, Y. S. (2014). Cryptococcus neoformans and Cryptococcus gattii, the etiologic agents of cryptococcosis. *Cold Spring Harb Perspect Med*, *4*(7), a019760. https://doi.org/10.1101/cshperspect.a019760

37. Lee, H., Chang, Y. C., & Kwon-Chung, K. J. (2005). TUP1 disruption reveals biological differences between MATa and MATalpha strains of Cryptococcus neoformans. *Mol Microbiol*, *55*(4), 1222-1232. https://doi.org/10.1111/j.1365-2958.2004.04458.x

38. Lin, J., Pham, T., Hipsher, K., Glueck, N., Fan, Y., & Lin, X. (2022). Immunoprotection against Cryptococcosis Offered by Znf2 Depends on Capsule and the Hyphal Morphology. *mBio*, *13*(1), e0278521. https://doi.org/10.1128/mbio.02785-21

39. Lin, X. (2009). Cryptococcus neoformans: morphogenesis, infection, and evolution. *Infect Genet Evol*, *9*(4), 401-416. https://doi.org/10.1016/j.meegid.2009.01.013

40. Lin, X., Jackson, J. C., Feretzaki, M., Xue, C., & Heitman, J. (2010). Transcription factors Mat2 and Znf2 operate cellular circuits orchestrating opposite- and same-sex mating in Cryptococcus neoformans. *PLoS Genet*, *6*(5), e1000953. https://doi.org/10.1371/journal.pgen.1000953

41. Lin, X., Nielsen, K., Patel, S., & Heitman, J. (2008). Impact of Mating Type, Serotype, and Ploidy on the Virulence of Cryptococcus neoformans. *Infection and Immunity*, *76*(7), 2923-2938. https://doi.org/doi:10.1128/iai.00168-08

42. Litvintseva, A. P., Marra, R. E., Nielsen, K., Heitman, J., Vilgalys, R., & Mitchell, T. G. (2003). Evidence of sexual recombination among Cryptococcus neoformans serotype A isolates in sub-Saharan Africa. *Eukaryot Cell*, *2*(6), 1162-1168. https://doi.org/10.1128/ec.2.6.1162-1168.2003

43. Liu, O. W., Kelly, M. J., Chow, E. D., & Madhani, H. D. (2007). Parallel beta-helix proteins required for accurate capsule polysaccharide synthesis and virulence in the yeast Cryptococcus neoformans. *Eukaryot Cell*, *6*(4), 630-640. https://doi.org/10.1128/EC.00398-06

44. Livak, K. J., & Schmittgen, T. D. (2001). Analysis of relative gene expression data using real-time quantitative PCR and the 2(-Delta Schnittger C(T)) Method. *Methods*, *25*(4), 402-408. https://doi.org/10.1006/meth.2001.1262

45. Lobo, S., Greentree, W. K., Linder, M. E., & Deschenes, R. J. (2002). Identification of a Ras palmitoyltransferase in Saccharomyces cerevisiae. *J Biol Chem*, *277*(43), 41268-41273. https://doi.org/10.1074/jbc.M206573200

46. Martinez, L. R., & Casadevall, A. (2007). Cryptococcus neoformans biofilm formation depends on surface support and carbon source and reduces fungal cell susceptibility to heat, cold, and UV light. *Appl Environ Microbiol*, *73*(14), 4592-4601. https://doi.org/10.1128/aem.02506-06

47. Maziarz, E. K., & Perfect, J. R. (2016). Cryptococcosis. *Infect Dis Clin North Am*, *30*(1), 179-206. https://doi.org/10.1016/j.idc.2015.10.006

48. McClelland, C. M., Chang, Y. C., Varma, A., & Kwon-Chung, K. J. (2004). Uniqueness of the mating system in Cryptococcus neoformans. *Trends Microbiol*, *12*(5), 208-212. https://doi.org/10.1016/j.tim.2004.03.003

49. Montoya, M. C., Magwene, P. M., & Perfect, J. R. (2021). Associations between Cryptococcus Genotypes, Phenotypes, and Clinical Parameters of Human Disease: A Review. *Journal of Fungi*, *7*(4), 260. https://www.mdpi.com/2309-608X/7/4/260

50. Mukaremera, L., & Nielsen, K. (2017). Adaptive Immunity to Cryptococcus neoformans Infections. *J Fungi (Basel)*, *3*(4). https://doi.org/10.3390/jof3040064

51. Nelson, B. N., Hawkins, A. N., & Wozniak, K. L. (2020). Pulmonary Macrophage and Dendritic Cell Responses to Cryptococcus neoformans [Review]. *Frontiers in Cellular and Infection Microbiology*, *10*. https://doi.org/10.3389/fcimb.2020.00037

52. Nichols, C. B., Ferreyra, J., Ballou, E. R., & Alspaugh, J. A. (2009). Subcellular localization directs signaling specificity of the Cryptococcus neoformans Ras1 protein. *Eukaryot Cell*, *8*(2), 181-189. https://doi.org/10.1128/ec.00351-08

53. Nichols, C. B., Ost, K. S., Grogan, D. P., Pianalto, K., Hasan, S., & Alspaugh, J. A. (2015). Impact of Protein Palmitoylation on the Virulence Potential of Cryptococcus neoformans. *Eukaryot Cell*, *14*(7), 626-635. https://doi.org/10.1128/EC.00010-15

54. Nielsen, K., Cox, G. M., Wang, P., Toffaletti, D. L., Perfect, J. R., & Heitman, J. (2003). Sexual cycle of Cryptococcus neoformans var. grubii and virulence of congenic a and alpha isolates. *Infect Immun*, *71*(9), 4831-4841. https://doi.org/10.1128/iai.71.9.4831-4841.2003

55. Ning, W., Jiang, P., Guo, Y., Wang, C., Tan, X., Zhang, W., Peng, D., & Xue, Y. (2020). GPS-Palm: a deep learning-based graphic presentation system for the prediction of S-palmitoylation sites in proteins. *Briefings in Bioinformatics*, *22*(2), 1836-1847. https://doi.org/10.1093/bib/bbaa038

56. Normile, T. G., & Del Poeta, M. (2022). Three Models of Vaccination Strategies Against Cryptococcosis in Immunocompromised Hosts Using Heat-Killed Cryptococcus neoformans Δsgl1 [Original Research]. *Frontiers in Immunology*, *13*. https://doi.org/10.3389/fimmu.2022.868523

57. Organization, W. H. (2022). *WHO fungal priority pathogens list to guide research, development and public health*

58. Ory, J. J., Griffith, C. L., & Doering, T. L. (2004). An efficiently regulated promoter system for Cryptococcus neoformans utilizing the CTR4 promoter. *Yeast*, *21*(11), 919-926. https://doi.org/10.1002/yea.1139

59. Pham, T., Li, Y., Watford, W., & Lin, X. (2023). Vaccination with a ZNF2(oe) Strain of Cryptococcus Provides Long-Lasting Protection against Cryptococcosis and Is Effective in Immunocompromised Hosts. *Infect Immun*, *91*(7), e0019823. https://doi.org/10.1128/iai.00198-23

60. Pierce, C. G., Uppuluri, P., Tristan, A. R., Wormley, F. L., Jr., Mowat, E., Ramage, G., & Lopez-Ribot, J. L. (2008). A simple and reproducible 96-well plate-based method for the formation of fungal biofilms and its application to antifungal susceptibility testing. *Nat Protoc*, *3*(9), 1494-1500. https://doi.org/10.1038/nport.2008.141

61. Rajasingham, R., Govender, N. P., Jordan, A., Loyse, A., Shroufi, A., Denning, D. W., Meya, D. B., Chiller, T. M., & Boulware, D. R. (2022). The global burden of HIV-associated cryptococcal infection in adults in 2020: a modelling analysis. *Lancet Infect Dis*, *22*(12), 1748-1755. https://doi.org/10.1016/S1473-3099(22)00499-6

62. Ramage, C. M., & Williams, R. R. (2003). Mineral uptake in tobacco leaf discs during different developmental stages of shoot organogenesis. *Plant Cell Rep*, *21*(11), 1047-1053. https://doi.org/10.1007/s00299-003-0628-3

63. Raudaskoski, M., & Kothe, E. (2010). Basidiomycete mating type genes and pheromone signaling. *Eukaryot Cell*, *9*(6), 847-859. https://doi.org/10.1128/EC.00319-09

64. Roach, K. C., Feretzaki, M., Sun, S., & Heitman, J. (2014). Unisexual reproduction. *Adv Genet*, *85*, 255-305. https://doi.org/10.1016/B978-0-12-800271-1.00005-6

65. Roberts, G. G., 3rd, Parrish, J. R., Mangiola, B. A., & Finley, R. L., Jr. (2012). High-throughput yeast two-hybrid screening. *Methods Mol Biol*, *812*, 39-61. https://doi.org/10.1007/978-1-61779-455-1_3

66. Rosen, L. B., Freeman, A. F., Yang, L. M., Jutivorakool, K., Olivier, K. N., Angkasekwinai, N., Suputtamongkol, Y., Bennett, J. E., Pyrgos, V., Williamson, P. R., Ding, L., Holland, S. M., & Browne, S. K. (2013). Anti-GM-CSF autoantibodies in patients with cryptococcal meningitis. *J Immunol*, *190*(8), 3959-3966. https://doi.org/10.4049/jimmunol.1202526

67. Roth, A. F., Feng, Y., Chen, L., & Davis, N. G. (2002). The yeast DHHC cysteine-rich domain protein Akr1p is a palmitoyl transferase. *J Cell Biol*, *159*(1), 23-28. https://doi.org/10.1083/jcb.200206120

68. Sabiiti, W., Robertson, E., Beale, M. A., Johnston, S. A., Brouwer, A. E., Loyse, A., Jarvis, J. N., Gilbert, A. S., Fisher, M. C., Harrison, T. S., May, R. C., & Bicanic, T. (2014). Efficient phagocytosis and laccase activity affect the outcome of HIV-associated cryptococcosis. *J Clin Invest*, *124*(5), 2000-2008. https://doi.org/10.1172/JCI72950

69. Santiago-Tirado, F. H., Peng, T., Yang, M., Hang, H. C., & Doering, T. L. (2015). A Single Protein S-acyl Transferase Acts through Diverse Substrates to Determine Cryptococcal Morphology, Stress Tolerance, and Pathogenic Outcome. *PLoS Pathog*, *11*(5), e1004908. https://doi.org/10.1371/journal.ppat.1004908

70. Severin, F. F., & Hyman, A. A. (2002). Pheromone induces programmed cell death in S. cerevisiae. *Curr Biol*, *12*(7), R233-235. https://doi.org/10.1016/s0960-9822(02)00776-5

71. Shen, W. C., Davidson, R. C., Cox, G. M., & Heitman, J. (2002). Pheromones stimulate mating and differentiation via paracrine and autocrine signaling in Cryptococcus neoformans. *Eukaryot Cell*, *1*(3), 366-377. https://doi.org/10.1128/ec.1.3.366-377.2002

72. Sobocińska, J., Roszczenko-Jasińska, P., Ciesielska, A., & Kwiatkowska, K. (2017). Protein Palmitoylation and Its Role in Bacterial and Viral Infections. *Front Immunol*, *8*, 2003. https://doi.org/10.3389/fimmu.2017.02003

73. Son, Y. E., Fu, C., Jung, W. H., Oh, S. H., Kwak, J. H., Cardenas, M. E., Heitman, J., & Park, H. S. (2019). Pbp1-Interacting Protein Mkt1 Regulates Virulence and Sexual Reproduction in Cryptococcus neoformans. *Front Cell Infect Microbiol*, *9*, 355. https://doi.org/10.3389/fcimb.2019.00355

74. Srikanta, D., Santiago-Tirado, F. H., & Doering, T. L. (2014). Cryptococcus neoformans: historical curiosity to modern pathogen. *Yeast*, *31*(2), 47-60. https://doi.org/10.1002/yea.2997

75. Stempinski, P. R., Smith, D. F. Q., & Casadevall, A. (2022). Cryptococcus neoformans Virulence Assay Using a Galleria mellonella Larvae Model System. *Bio Protoc*, *12*(15). https://doi.org/10.21769/BioProtoc.4480

76. Sun, S., Coelho, M. A., David-Palma, M., Priest, S. J., & Heitman, J. (2019). The Evolution of Sexual Reproduction and the Mating-Type Locus: Links to Pathogenesis of Cryptococcus Human Pathogenic Fungi. *Annu Rev Genet*, *53*, 417-444. https://doi.org/10.1146/annurev-genet-120116-024755

77. Sun, S., Priest, S. J., & Heitman, J. (2019). Cryptococcus neoformans Mating and Genetic Crosses. *Curr Protoc Microbiol*, *53*(1), e75. https://doi.org/10.1002/cpmc.75

78. Swearingen, K. E., Hoopmann, M. R., Johnson, R. S., Saleem, R. A., Aitchison, J. D., & Moritz, R. L. (2012). Nanospray FAIMS fractionation provides significant increases in proteome coverage of unfractionated complex protein digests. *Molecular & Cellular Proteomics*, *11*(4).

79. Szewczyk, E., & Krappmann, S. (2010). Conserved regulators of mating are essential for Aspergillus fumigatus cleistothecium formation. *Eukaryot Cell*, *9*(5), 774-783. https://doi.org/10.1128/ec.00375-09

80. Viviani, M. A., Esposto, M. C., Cogliati, M., Montagna, M. T., & Wickes, B. L. (2001). Isolation of a Cryptococcus neoformans serotype A MATa strain from the Italian environment. *Med Mycol*, *39*(5), 383-386. https://doi.org/10.1080/mmy.39.5.383.386 Yoneda, A., & Doering, T. L. (2008). Regulation of Cryptococcus neoformans capsule size is mediated at the polymer level. *Eukaryot Cell*, *7*(3), 546-549. https://doi.org/10.1128/ec.00437-07

81. Wang, L., Zhai, B., & Lin, X. (2012). The link between morphotype transition and virulence in Cryptococcus neoformans. *PLoS Pathog*, *8*(6), e1002765. https://doi.org/10.1371/journal.ppat.1002765

82. Wickes, B. L. (2002). The role of mating type and morphology in Cryptococcus neoformans pathogenesis. *Int J Med Microbiol*, *292*(5-6), 313-329. https://doi.org/10.1078/1438-4221-00216

83. Xu, X., Lin, J., Zhao, Y., Kirkman, E., So, Y. S., Bahn, Y. S., & Lin, X. (2017). Glucosamine stimulates pheromone-independent dimorphic transition in Cryptococcus neoformans by promoting Crz1 nuclear translocation. *PLoS Genet*, *13*(9), e1006982. https://doi.org/10.1371/journal.pgen.1006982

84. Xue, C., Tada, Y., Dong, X., & Heitman, J. (2007). The human fungal pathogen Cryptococcus can complete its sexual cycle during a pathogenic association with plants. *Cell Host Microbe*, *1*(4), 263-273. https://doi.org/10.1016/j.chom.2007.05.005

85. Yount, J. S., Zhang, M. M., & Hang, H. C. (2011). Visualization and Identification of Fatty Acylated Proteins Using Chemical Reporters. *Curr Protoc Chem Biol*, *3*(2), 65-79. https://doi.org/10.1002/9780470559277.ch100225

86. Yu, C. H., Sephton-Clark, P., Tenor, J. L., Toffaletti, D. L., Giamberardino, C., Haverkamp, M., Cuomo, C. A., & Perfect, J. R. (2021). Gene Expression of Diverse Cryptococcus Isolates during Infection of the Human Central Nervous System. *mBio*, *12*(6), e0231321. https://doi.org/10.1128/mBio.02313-21

87. Zhai, B., Wozniak, K. L., Masso-Silva, J., Upadhyay, S., Hole, C., Rivera, A., Wormley, F. L., Jr., & Lin, X. (2015). Development of protective inflammation and cell-mediated immunity against Cryptococcus neoformans after exposure to hyphal mutants. *mBio*, *6*(5), e01433-01415. https://doi.org/10.1128/mBio.01433-15